Crystallization control via membrane distillation-crystallization: a review

Marie-Charlotte Sparenberg[1,*], Sara Chergaoui[1], Vida Sangsefidi[1], Patricia Luis[1]
[1]Materials and Process Engineering (iMMC-IMAP), UCLouvain, Place Sainte Barbe 2, 1348 Louvain-la-Neuve, Belgium
[*]Corresponding author: marie-charlotte.sparenberg@uclouvain.be; Tel.: +32 10 47 24 93

Abstract: Membrane distillation-crystallization is a promising method potentially able to outperform the conventional crystallization processes in terms of crystallization control and product quality. This review gives a comprehensive overview of the current research addressing membrane distillation-crystallization and its advantages for crystallization control. More specifically, this work focuses on the impact of different parameters on crystal morphology and quality. The research papers about membrane distillation-crystallization reporting control of crystal habit, polymorphism, crystal size distribution, coefficient of variation, crystal yield, crystal purity, nucleation rate, growth rate and induction time are comprehensively reviewed and discussed. The methods and instruments of measure are systematically specified, and common guidelines are proposed to adjust discrepancies. Finally, the review indulges in a critical assessment of the challenges faced by membrane distillation-crystallization.

Keywords: Membrane distillation, membrane crystallization, crystallization control, crystal morphology, crystal size distribution.

1. Introduction

Crystallization is an age-old separation and purification process but still central in process engineering, presenting a wide range of applications, going from the production of basic materials to sophisticated pharmaceuticals [1], [2]. Compared to other purification processes, crystallization offers a high recovery rate, the recovery of high-quality solid and liquid products, a high yield, low energy requirements, good operability and good stability [2], [3]. Crystallization is generally the final step in a production process, and its control is of crucial importance. This is especially true nowadays because of the increasingly strict criteria in the industry in terms of specifications and quality [4]. However, although it has been applied for years, a lot of research still focuses on the understanding and control of the crystallization processes [5]. There is still a lack of knowledge about the fundamental mechanisms of crystallization [6], and crystallization control is difficult as the process is dependent on many inter-related factors such as the type of equipment, the operating conditions and the nature of the crystal to be crystallized. This led to the development of several crystallization techniques, always seeking to improve the performances, efficiency, and characteristics of the produced crystals.

Membrane processes have driven much attention in the last decade and are believed to be able to tackle some challenges encountered in conventional crystallization processes [7]. Several techniques exist, but they invariably rely on the use of a membrane to help the separation and perform a well-controlled crystallization. The reverse osmosis technique has been investigated for crystallization purposes but many issues about membrane fouling and scaling were reported [7]. Other membrane processes such as ion exchange and pervaporation have also been studied but in a very limited number of studies [7], [8]. On the other hand, membrane distillation was also considered for crystallization, and the number of publications is constantly increasing [9], [10], as shown in Figure 1.

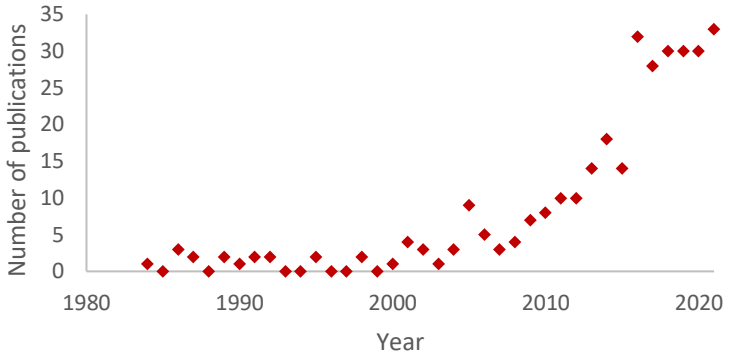

Figure 1: The increasing trend of the number of publications per year including « Membrane AND distillation AND crystallization » in the title, abstract, and key words of scientific journals, Scopus, August 2021.

Membrane distillation is a separation technique that enables a non-dispersive contact between two streams through a membrane, which allows distillation of the feed stream. Figure 2 displays the five most studied configurations for membrane distillation, illustrated with membranes in the form of thin tubes or hollow fibers, but the principle remains the same with other forms such as flat sheet membranes. The detailed working principle is depicted: the feed stream flows at one side of the membrane and the volatile species evaporate through the hydrophobic porous membrane, leading to progressive concentration of the feed solution [11].The incentive for evaporation differs depending on the configuration: direct contact membrane distillation (DCMD) uses a thermal gradient [12], osmotic membrane distillation (OMD) uses a concentration gradient [13], sweep gas membrane distillation (SGMD) uses a sweeping gas [14], air gap membrane distillation (AGMD) uses a temperature gradient combined with an air gap [15], and vacuum membrane distillation (VMD) uses vacuum [16]. The term "membrane distillation-*crystallization*" is employed when the solution is concentrated up to supersaturation and hence the system attains suitable conditions for crystallization [11]. Note that depending on the process, the feed solution can either flow in the lumen (inside the fibers) or in the shell (outside the fibers), and that these configurations were occasionally slightly adapted (*e.g.* submerged VMD) [17].

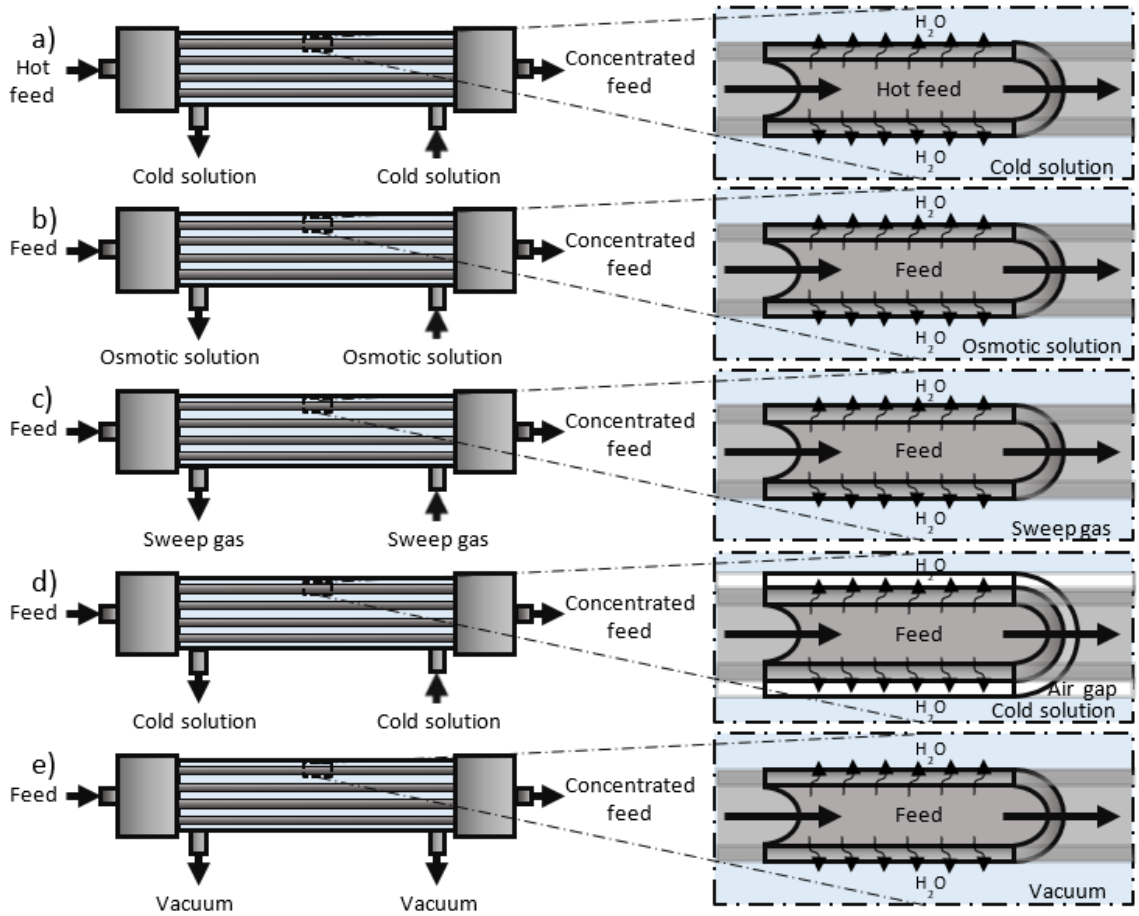

Figure 2: Different membrane distillation configurations illustrated with the feed solution flowing in the membrane fibers: a) direct contact membrane distillation (DCMD), b) osmotic membrane distillation (OMD), c) sweep gas membrane distillation (SGMD), d) air gap membrane distillation (AGMD), e) vacuum membrane distillation (VMD).

The advantages of membrane distillation for crystallization are numerous: possibility to work at high concentration, improved fluid distribution, heterogeneous nucleation, high surface to volume ratio, possibility to disassociate nucleation from growth, easy control of solvent removal hence controlled supersaturation, complete rejection of nonvolatile solutes, possibility of low operating temperatures, *etc*. [7], [18]. However, even though membrane distillation-crystallization offers several advantages, there are also some drawbacks coming with this kind of technology. The main disadvantage is related to the membrane itself, which adds a resistance to mass transfer and hence lowers the water flux through the membrane [19], this is, lowers the evaporation rate. Another important drawback is the scaling phenomena on top of the membrane that can lead to a reduction of flux or even complete membrane blockage.

This paper provides an overview of the current state of the art in the field of membrane distillation-crystallization. The article first provides a quick reminder about the crystallization phenomenon and its underlying parameters. The core of this work consists in a comprehensive review about the different studies on crystallization control using membrane distillation-crystallization. The research about the impact of membrane distillation-crystallization on several important crystal parameters such as crystal size distribution, crystal purity and yield is summarized. The methods and instruments of measure are systematically specified, and common guidelines are proposed to adjust discrepancies. Finally, section 5 highlights the current advances and challenges in this field of work.

2. Crystallization principles

As illustrated in Figure 3, regardless of the technology, crystallization can usually be initiated in two different ways: either the feed solution is cooled, or the feed solution is concentrated [7]. These changes in solubility transform the undersaturated solution into a saturated solution once the solubility curve is crossed. Crystallization can then be induced by seeding, or can occur spontaneously if the spontaneous nucleation curve is crossed. Note that the solubility curve depends on thermodynamics, whereas the spontaneous nucleation curve depends on kinetics and is therefore process-dependent [4]. The addition of an anti-solvent reduces the solubility of the solute and hence initiates crystallization in a third way [20].

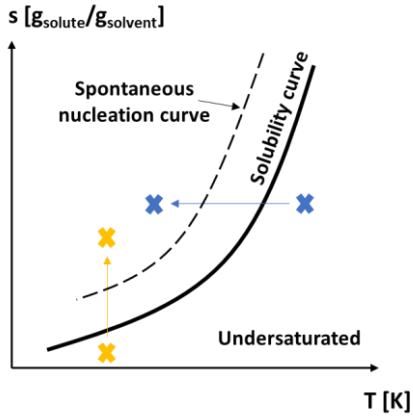

Figure 3: Typical solubility curves showing the amount of solute that can dissolve in a given amount of solvent, at a certain temperature. The paths for cooling and concentrative crystallization are illustrated.

In membrane crystallization, different supersaturation paths can be followed depending on the technique [7]: amongst others, pressure-driven membrane processes such as ultrafiltration, nanofiltration and reverse osmosis generate supersaturation by pressurizing and hence concentrating the solution via selective mass transfer [21]. Anti-solvent membrane crystallization uses an anti-solvent to change the solubility of the feed solution and reach supersaturation [22]. Solid hollow fiber cooling crystallization reduces the feed temperature to induce crystallization via the cooling path [23].

In membrane *distillation*-crystallization, the subject of this review, it is mainly the evaporative path that is followed: the feed solution is concentrated up to supersaturation via solvent evaporation [24]. Note that the DCMD configuration combines mass and heat transfer, and is thus taking both cooling and evaporative paths at the same time. When supersaturation is finally reached, nucleation is generally fast thanks to the presence of the membrane which acts as a heterogeneous nucleation site [25]–[28]. It is interesting to note that the conditions at the membrane are not the same than in the bulk because of polarization phenomena (see Figure 4Figure 4 : Typical temperature and concentration profiles in membrane distillation-crystallization.). The resulting lower temperature and higher concentration at the surface of the membrane also promote crystallization on the membrane rather than in the bulk solution. When nucleation occurs on the membrane, crystal detachment via flow shear stress is usually desired in order to conduct the nuclei to a separate crystallizer for further growth [29]. This intends to reduce the risk of membrane scaling and blockage. Finally, the crystals are recovered after a filtration step.

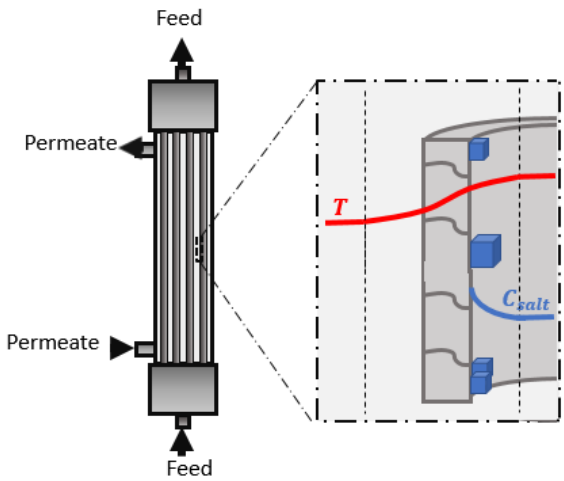

Figure 4 : Typical temperature and concentration profiles in membrane distillation-crystallization.

3. Crystallization control pathways in membrane distillation-crystallization

The quality of crystals is measured in terms of uniformity in shape, size, structure, and purity [30]. As these properties are influenced by the crystallization process, well-controlled crystallization conditions are of uttermost importance. Membrane distillation-crystallization is believed to provide a better control than conventional processes, especially thanks to the precise regulation of supersaturation, the possibility of separated nucleation and growth, the variety of possible nucleation-inducing surfaces, *etc.* [3], [7], [24]–[26], [31]–[35] This section gives an overview of the membrane distillation-crystallization studies that report the influence of process parameters on crystal quality and crystallization kinetics.

3.1 Crystal morphology

The crystal morphology is usually described via the crystal habit and polymorphism. The crystal habit is a visual characteristic expressing the external shape of the crystal. Polymorphism describes the existence of crystals composed of the same molecules, but having a different internal structure, and usually also a different external shape (habit). Note that a same compound can present different crystal habits that are not due to polymorphic changes [36]. Either way, the crystal morphology is very dependent on the crystallization conditions, and membrane distillation-crystallization could offer an effective control and hence outperform conventional crystallization processes. Table 1 summarizes the main studies reporting the influence of different variables on the crystal morphology obtained using membrane distillation-crystallization. The typical instrument of measure is the optical microscope but Scanning Electron Microscopy (SEM) can also be used and offers a higher resolution and magnification.

Several authors studied the impact of the **crystallization technology** on the crystal morphology. Lu, *et al.*, [37] compared membrane distillation-crystallization with conventional vacuum evaporative crystallization and obtained agglomerated crystals with clear helical defects with the latter, but regular cubic shaped crystals with membrane crystallization. Weckesser, *et al.*, [38] similarly reported irregularly grown crystals with vacuum evaporative crystallization, and finely-developed cubic-shaped crystals with membrane distillation-crystallization. In addition, Jiang, *et al.*, [39] reported sharper edges with membrane distillation-crystallization than with conventional cooling crystallization. Membrane distillation-crystallization seems thus competitive in terms of crystal morphology compared to conventional technologies.

There are different variables that can be tuned in membrane distillation-crystallization for crystal morphology control. Di Profio, *et al.*, [40] demonstrated that the precise **control of supersaturation** in membrane distillation-crystallization makes the selective crystallization of a certain

paracetamol polymorph possible. Indeed, they managed to crystallize form II at low transmembrane **flux**, and form I at intermediate flux. The form I had an elongated prismatic habit at low supersaturation and a well-developed prismatic habit at higher supersaturation. Di Profio, *et al.*, [41] also reported the influence of evaporation rate on the selective polymorphic yield of glycine. Quist-Jensen, *et al.,* [42] studied vacuum membrane distillation-crystallization for lithium recovery and observed that the crystals can be recovered in cubic or orthorhombic polymorphic structures depending on the process conditions. Indeed, they report that the cubic form is present at low **temperatures** but disappears completely at temperatures higher than 64°C. Jiang, *et al.*, [43] studied NaCl membrane distillation-crystallization and observed smooth surfaces at low temperature but an increasing number of surface defects and attachment at higher temperature. Curcio, *et al.*, [44] reported an elongation of tetragonal hen egg white lysozyme when increasing the **flow rate**. More recently, the effect of the **membrane** on the crystal morphology was also investigated. Macedonio, *et al.*, [45] noted a higher regularity in shape with a PVDF-Bi_2Se_3 membrane than with an ordinary pristine PVDF membrane. In a less studied membrane distillation-crystallization mode, Ji, *et al.*, [46] reported a selective growth towards aragonite phase when using DCMD crystallization with **microwaves** irradiation. Finally, Ye, *et al.*, [47] showed that SO_4^{2-} **impurities** affected Na_2CO_3 crystals, which went from a prismatic to a triclinic structure. More precisely, they showed that the impurities do not affect the nucleation step on the membrane, but only act during growth. Other studies [47]–[50] also report morphology changes in the presence of impurities, hence the crystallization process should be designed with a potential pre-treatment step.

Table 1: Main studies reporting crystal morphology control via membrane distillation-crystallization.

Target recovery	**Membrane**	**Config.**	**Morphology**	**Instrument of measure**	**Control variable**	**Ref.**
Glycine	Hollow fiber, PP	Static and dynamic OMD	Two morphologies depending on the stripping solution concentration (driving force) and feed velocity.	Optical microscope	Driving force, feed velocity.	[41]
NaCl	Hollow fiber, PP	VMD	Helical surface and agglomeration with vacuum evaporative crystallization, but uniform cubic shape with VMD. Smoother morphology at high ethanol glycol (EG) concentration.	Optical microscope, SEM	Crystallization technology, composition.	[37]
NaCl	Tubular, PP	SGMD	Irregular crystals (conventional vacuum evaporation) versus finely developed cubic crystals (SGMD).	/	Crystallization technology	[38]
KNO_3	Hollow fiber, PP	DCMD	Crystal habit sharper in membrane assisted cooling mode with optimized profiles.	/	Crystallization technology	[39]
Paracetamol	Hollow fiber, PP	Static OMD	Form I and/or II depending on flux. Well-developed / elongated form I, depending on supersaturation.	Optical microscope	Flux	[40]
LiCl	Hollow fiber, PP	VMD	Cubic (at low T) and orthorhombic (dominant).	Optical microscope	Temperature	[42]
NaCl	Hollow fiber, PP	VMD	Cubic. Smooth surface at low viscosity and temperature. Increasing temperature leads to increasing surface defect and attachment.	SEM	Temperature, diffusion	[43]
Hen egg white	Hollow fiber, PP	OMD	Elongation of the crystal length when increasing the flow rate.	Optical microscope	Flow rate	[44]
NaCl	Flat sheet, hybrid PVDF-Bi_2Se_3	DCMD	Cubic form. Higher regularity in shape with PVDF-Bi2Se3.	Optical microscope	Membrane composition	[45]
$CaCO_3$	Flat sheet, PVDF	DCMD	Selective growth towards aragonite phase with microwaves.	SEM	Microwaves	[46]
Na_2CO_3	Hollow fiber, PP	OMD	Prismatic structure. SO_4^{2-} impurities lead to triclinic crystals.	Optical microscope	Feed composition	[47]

Na_2CO_3	Hollow fiber, PP	OMD	Hexagonal shapes. Change to monoclinic and triclinic shapes with impurities.	Optical microscope	Feed composition	[48]
NaCl	Hollow fiber, PP	DCMD	Cubic block-like form. With strontium: more rectangular.	Optical microscope	Feed composition	[49]
NaCl	/	DCMD	Cubic without ions, elongated with ions (i.e., depending on pre-treatment).	Optical microscope	Feed composition	[50]
NaCl	Hollow fiber, PP	VMD	High viscosity: homogeneous, ideal cubic with smooth faces. Low viscosity: more fragmented polynuclear growth.	Optical microscope, SEM	Viscosity	[51]
CBZ-SAC	Hollow fiber, PP	DCMD	Increasing transmembrane flow rate decreases the amount of CBZ I and increases CBZ IV.	PXRD	Transmembrane flow rate	[52]

3.2 Crystal size distribution

Crystals can be characterized by a size distribution (CSD) describing the number of crystals within defined size intervals. As the crystals are 3-dimentional particles, the concept of equivalent sphere diameters is used to simplify the particle size definition. The earliest measurement techniques include basic sieving but this is very time-consuming and delivers the results with delay. The current most used techniques include image analysis, laser diffraction and Coulter counters. The first can be realized in-situ and provides an additional shape information but is limited to dilute slurries. The second is quick and convenient but needs to translate the light diffraction measurements into a crystal size distribution, which needs additional hypotheses. The latter is very accurate but only allows a relatively narrow size range [2]. It is important to note here that these different techniques give different information about the particle size. For example, sieving separates the particles according to their linear dimensions, whereas Coulter counters measure the volume of the particles [53]. Accordingly, the different measurement techniques usually use different definitions of the equivalent sphere diameter (an equivalent sphere with the same length/weight/volume/area … as the particle). Therefore, the different techniques will not provide exactly the same equivalent diameter. This equivalent sphere diameters concept can be especially misleading when the particle differs significantly from a sphere; for needles and platelets for example. Therefore, researchers need to be careful when selecting the size measurement technique when comparing different studies.

Once measured, the CSD is often defined by the median diameter and the coefficient of variation. This method was proposed by Powers (1948) for use in the sugar industry [54] and can be applied if the cumulative sizes between 10 and 90 percent plotted on an arithmetic-probability graph lie on a straight line. The coefficient of variation (CV) indicates the spread of the size distribution around the mean size [55] and is defined as the ratio of the standard deviation to the mean. In the case of a standard normal distribution, it can be calculated as [50], [54], [56]–[59] :

$$CV = 100\% \frac{L_{84\%} - L_{16\%}}{2L_{50\%}} \qquad 1$$

With L the crystal length at which the cumulative distribution function equals the indicated percentage. Several authors [60]–[65] calculate the coefficient of variation as $CV = 100\% \frac{L_{80\%} - L_{20\%}}{2L_{50\%}}$ without reference or with a reference pointing to [54]. However, [54] defines CV as first mentioned hence we recommend using the first definition which is more precise.

A narrow crystal size distribution (CSD) is a typical quality criterion as it affects processing steps such as filtration and storage [50], [66]. Therefore, all crystallization processes strive to produce crystals with a coefficient of variation as low as possible. Membrane distillation-crystallization stands out from the **conventional** crystallization technologies such as the Mixed Suspension-Mixed Product Removal (MSMPR) crystallization technique, which usually yields crystals with a coefficient of variation

of 50%, whereas the membrane distillation-crystallization literature reports substantially lower CVs. Some authors specifically compared experimentally the crystal size distribution of membrane distillation-crystallization and other conventional processes. Lu, *et al.*, [37] showed that conventional vacuum evaporative crystallization yields crystals with a higher average size but higher CV than membrane distillation-crystallization. Jiang, *et al.*, [39] reported higher mean crystal size and lower CV for membrane crystallization compared to conventional cooling crystallization. Qu, *et al.*, [67] reported a more uniform CSD but a lower proportion of coarse crystals in vacuum membrane distillation-crystallization than in evaporative crystallization.

As for the impact of membrane distillation-crystallization parameters, several authors investigated the influence control variables on the crystal size distribution (Table 2). Many of them witnessed increasing CV and mean diameters with **time** [39], [44], [57], [68]–[71]. However, Quist-Jensen, *et al.*, [72] reported a decrease in Na_2SO_4 mean diameter with time and explained this by the occurrence of a secondary nucleation in the crystallization plant. Cui, et al., [64] explained similarly their increase and then decrease of NaCl mean diameters with time. Furthermore, they observed that this effect is more pronounced for the membrane with the highest **flux**. Macedonio, et al., [45] studied the influence of **membrane composition** by adding Bi_2Se_3 fillers in PVDF membranes. This also led to a higher uniformity of the NaCl CSD and a lower CV. Perrotta, *et al.*, [62] studied the influence of graphene loading in PVDF flat sheet membranes and concluded that a graphene loading leads to a more uniform NaCl CSD and lower CV than pristine PVDF thanks to the assisted water exclusion. Frappa, *et al.*, obtained more uniform NaCl crystals with graphene and bismuth telluride PVDF membranes compared with pristine PVDF membranes [59].
Other process parameters can have an influence on the crystal size distribution and coefficient of variation. Shin, *et al.*, [73] studied sea salt crystallization using DCMD crystallization and reported that the average crystal size is larger at low **flow rate**. This was also observed in [42], [58], [74] (LiCl, NaCl and NaCl crystallization, respectively) and explained either by the increased residence time for growth in the crystallizer or by the fact that crystal growth was mainly limited by the resistance to integration into the crystal lattice. However, other authors [63], [65] ($MgSO_4$ and $CaCO_3$ crystallization, respectively) report an increase of mean diameter at increasing flow rate, which is explained by particle diffusion limitation in the latter study. Macedonio, *et al.*, [75] studied the crystal size distribution and the coefficient and variation of NaCl crystals produced with direct contact membrane distillation-crystallization. They noted an increase of mean diameter with time, and the **presence of humic acid** led to lower mean diameters and higher coefficients of variation. They also reported lower CV and mean diameters at higher feed **temperatures**. [57], [65], [74] similarly reported decreasing NaCl crystal size at increasing temperature in DCMD. In contrast, Ali, *et al.*, [58] also working on NaCl DCMD crystallization, reported increasing mean diameters but decreasing CV with increasing temperature for PVDF membranes and no clear trend for PP membranes. It is interesting to note that for a same product (NaCl), same membrane configuration (DCMD) and same membrane material (PVDF), [57], [58] give opposite results. Bouchrit, *et al.*, [76] reported increasing CV and mean diameter with temperature when producing Na_2SO_4 crystals by direct contact membrane distillation. Finally, Bouchrit, *et al.*, [76] used **seeding** instead of spontaneous crystallization and reported a decreasing coefficient of variation explained by lower appearance of small crystals. Edwie, *et al.*, [77] showed that the CSD of crystals formed under natural **cooling** of the crystallization vessel show larger average sizes compared to rapid cooling because of the promoted diffusion and growth over additional nucleation.

Using hybrid membrane distillation techniques, some more variables can be manipulated. For example, Tong, *et al.*, [78] showed that low **stirring rate** and low **aeration** in submerged vacuum membrane distillation-crystallization leads to higher mean crystal size. The CSD was shown to be wider with intensive aeration, likely because of the formation of smaller-sized crystals. Finally, Ji, *et al.*, [46] showed that **microwave radiation** makes the CSD mode uniform during NaCl crystallization.

In this section, the review of the literature identified several variables that can have an effect on the crystal size distribution. Of course, depending on the salt to be crystallized and on the process conditions, these variables may influence the CSD in various ways. Therefore, each crystallization system must be optimized individually, taking into account its own specificities.

Table 2: Main studies reporting crystal size distribution (CSD) control via membrane distillation-crystallization.

Target recovery	Membrane	Config.	CSD	CV	Instrument of measure	Control variable	Ref.
NaCl	Hollow fiber, PP	VMD	Average size of 100 µm for VEC, and 50 µm for MDC. Average size from 49.09 to 162 µm with decreasing EG concentration.	46.2% for VEC, and 38.07% for MDC. Lowest CV (31.04%) at highest EG concentration.	Optical microscope, SEM, image analysis software	Feed composition, technology	[37]
KNO_3	Hollow fiber, PP and flat sheet PVDF	DCMD	Mean crystal sizes were 548, 678 and 655 µm with natural cooling, membrane and rapid cooling crystallization.	55.4% with conventional cooling crystallization, and 33.9% in DCMD. Increases with time.	Particle analyzer (Mastersizer 2000)	Technology, time	[39]
LiCl	Hollow fiber, PP	VMD	Mean diameter: 83-139 µm at 38°C. Decreases with increase in flow rate at that temperature.	/	Optical microscope, camera	Flow rate	[42]
NaCl	Hollow fiber, PP	VMD	Mean crystal size higher with lean EG solutions (237 to 299 µm) than with rich EG solutions (49 to 54 µm).	Increase of temperature transfers the maximum CV from the lean EG solution to the rich EG solution.	Optical microscope, image analysis software	Temperature, solvent composition	[43]
Hen egg white	Hollow fiber, PP	OMD	Mean diameter increased with time.	CSD broadens with time.	Optical microscope	Time	[44]
NaCl	Flat sheet, hybrid PVDF-Bi_2Se_3	DCMD	CSD more uniform with Bi_2Se_3 additives in the membrane. Mean diameter: 507-747 µm PVDF-Bi_2Se_3 vs 299-526 µm pristine-PVDF.	36-44% PVDF-Bi_2Se_3 vs 40-63% pristine-PVDF.	/	Membrane composition	[45]
NaCl and $CaCO_3$	Flat sheet, PVDF	DCMD	CSD more uniform thanks to microwaves.	Standard deviation of NaCl crystals with and without microwaves: 61.10, 91.07.	SEM, image analysis (Nano Measurer, ImageJ)	Micro-wave	[46]
NaCl	/	DCMD	Mean diameter: 16.32 to 65.1 µm. Humic acid leads to lower mean diameter. Higher temperature leads to lower mean diameter.	CV: 25 to 67.19%. Humic acid leads to higher CV. Higher temperature leads to lower CV.	Optical microscope, camera	Time, feed temperature, humic acid concentration.	[50]
NaCl	Hollow fiber, PP	VMD	CSD more uniform than conventional non-MCr.	High viscosity leads to narrower CSD.	Optical microscope, camera, SEM, image analysis software	Viscosity, technology	[51]

NaCl	Hollow fiber, PVDF	DCMD	Average crystal size decreases from 87.40 µm to 48.82 µm with increasing feed temperature. CSD increases and broadens with time.	CV around 30-38%. No conclusion about the temperature. CSD increases and broadens with time.	Optical microscope, camera, image analysis software (Image-Pro Plus 7)	Temperature, time	[57]
NaCl	Hollow fiber, PP and PVDF	DCMD	Mean diameter decreased with increasing feed flow rate. Mean diameter increased with increasing temperature when using PVDF membranes.	CV decreased with increasing temperature. No conclusion about flow rate.	Optical microscope, camera, Image J	Temperature, flow rate	[58]
NaCl	Flat sheet, PVDF modified	DCMD	Larger mean diameter with pristine PVDF (65.1 µm), lower with modified membranes (~17 µm).	43.1-54.2% with PVDF/Bi_2Te_3 (0.5%), 36.7-44.2% with PVDF/Graphene (0.5%), 48.4-77.1% with PDVF.	Optical microscope	Membrane composition	[59]
NaCl	Flat sheet PVDF + graphene	DCMD	CSD more uniform with PVDF filled with 5% graphene loading.	PVDF with 5% graphene loading exhibits lowest CV (26.7%). PVDF with 0.5% graphene loading 32.2%. PVDF with 10% of graphene loading 35.8%. PVDF: 48.1%	/	Membrane composition	[62]
$MgSO_4$	Hollow fiber, PDVF	DCMD	Mean diameter increases from 367.2 µm at lower flow rate to 589.2 µm at higher flow rate.	CV around 30.52% to 41.44%. No conclusion about flow rate.	Optical microscope	Flow rate	[63]
NaCl	Flat sheet, Hyflon/ PVDF	DCMD	Mean diameter values are around 22.85 to 40.18. Increases with time, and then decreases. Effect more pronounced for the membrane with the highest flux.	CV around 35% to 50%, no conclusion about time nor membrane type.	Optical microscope	Time, membrane composition	[64]
$CaCO_3$ and NaCl	Hollow fiber, PP	DCMD	Increasing feed cross flow velocity increases mean crystal size. Increasing the crystallizer temperature lowers the mean crystal size.	At higher feed cross flow velocity, CV increased to 17.3% from 15.9 and 15.4%. CV increases with increasing crystallizer temperature.	/	Feed cross flow velocity, temperature	[65]
$MgSO_4$	Hollow fiber, PP	VMD	CSD more uniform but lower proportion of coarse crystals in VMD than in evaporative crystallization.	/	Particle analyzer (Mastersizer 2000)	Technology	[67]
Na_2SO_4	Hollow fiber, PP	DCMD	Mean crystal size increased from 84.5 µm to 170 µm.	23 to 40% depending on residence time.	Optical microscope, image processing software	Time	[68]

NaCl	Hollow fiber, PVDF	DCMD	Median size increases from ~10 to ~350 µm with time.	/	Particle analyzer (Mastersizer 2000)	Time	[69]
NaCl	Hollow fiber, PP	DCMD	Average size increase with time from ~40 to ~70 µm.	35-40% CV in general.	Optical microscope, camera	Time	[70]
Na_2SO_4 and NaCl	Flat sheet, PVDF	DCMD	73.3 to 79.2 µm average size increasing with time.	10.1 to 17.1% increasing with time.	Coulter counter	Time	[71]
Na_2SO_4	Hollow fiber, PP	DCMD	Mean diameter decreasing with time from 435.93 µm to 521.03 µm.	34.9 to 46.8%.	Optical microscope	Time	[72]
Sea salt	Hollow fiber, PVDF	DCMD	Average crystal size larger at low flow rate.	/	SEM	Flow rate	[73]
NaCl	Hollow fiber, PVDF	DCMD	Mean crystal size increases from 138.9 to 216.5 µm with decreasing feed flow rate, and from 188.1 to 209.9 µm with decreasing temperature.	/	Particle analyzer (Mastersizer 2000)	Feed flow rate, temperat ure	[74]
Na_2SO_4	Flat sheet, PVDF	DCMD	Mean size: 44.68 to 108.7 µm at temperatures from 40°C to 70°C. Mean size decreases with seeding (99.57 µm at 70°C).	12.2 to 40.6% at temperatures from 40°C to 70°C. CV decreases with seeding (33% at 70°C).	Laser diffraction particle size analyzer	Temperat ure, seeding	[76]
NaCl	Hollow fiber, PVDF modifie d	DCMD	CSD formed under natural cooling show larger average sizes (225 µm) compared to rapid cooling (85 µm).	/	Optical microscope, camera, image analysis software (Image-Pro Plus 7)	Time, cooling rate	[77]
NaCl	Hollow fiber, PTFE	Subm erged VMD	Higher average size at lower stirring rate (442.1 vs 317.1 µm) and lower aeration (389.4 vs 305.7 µm).	Wider CSD with intensive aeration.	Particle analyzer (Mastersizer 2000)	Stirring rate, aeration	[78]
NaCl	Tubular, PP	DCMD	Bimodal, mean diameter 46 and 224 µm, then 38 and 272 µm at higher local supersaturation.	/	Laser Light Scattering	Supersatu ration	[79]
NaCl, KCl	Hollow fiber, PP	DCMD	Average size of 900 µm for NaCl, 2000 µm for KCl.	/	Optical microscope	Feed compositi onpuri	[80]

3.3 Crystal yield

Crystal yield is an undeniably important variable when designing a crystallization process as it will determine its economic viability. Nonetheless, except for Tan *et al.* [81], who reported a phosphate recovery of about 82% and Quist-Jensen, et al., [82] who reported a phosphorus recovery of around 60%, which they claimed higher than the 40% removal attainable with a fluidized bed reactor under the same conditions, membrane distillation-crystallization studies still report crystal yield values that are quite low, compared to the conventional crystallization yield of around 80%. Weckesser, *et al.*, [38] reported a ratio between the produced salt mass and the mass of remaining mother liquor of about 1 to 2%. Zou, *et al.*, [78] reported a recovery of 31.85 out of the 100 g NaCl initially dissolved when using optimal process conditions. Bouchrit, *et al.*, [76] studied membrane crystallization for mineral recovery from Na_2SO_4 solutions, and reported a water recovery ratio of 80%, and a salt production of about 38%

of the initial dissolved salts. Kim, *et al.*, [65] report a solid production rate of 2.72 kg/m2/day. Ali, *et al.*, [58] reported 16.5 kg NaCl recovery per m^3 of produced water. Luo, *et al.*, [83] used membrane distillation as a concentration technology, and induced crystallization using solid hollow fiber cooling crystallization. They obtained a crystal yield of 64 g NaCl per kg of feed. Julian, *et al.*, [84] used submerged vacuum membrane distillation-crystallization for inland brine water treatment and reported a maximum of 16.14 g crystals produced, compared to a theoretical amount of 35.9 g.

The low yield observed with membrane distillation-crystallization could be explained by the scale of the processes: at lab scale, considerably large amounts of the salt solution is lost in the process, but this could be avoided at a larger scale, yet to be investigated. Thus far, Ji, *et al.*, [70] used a bench-scale membrane crystallization plant and produced 21 kg/m^3 of NaCl crystals from synthetic RO concentrates and reported 90% water recovery factor. They also noted a reduction of 20% on the salt yield when using RO brines from natural seawater. Anisi, *et al.*, [85] also studied membrane distillation-crystallization at bench scale, and they reported a 27% ratio between the resulting yield to that of the theoretical one. Another reason for the low yield observed with membrane distillation-crystallization could be that no study was yet entirely dedicated to increase the yield of the process. The current studies are still exploring all the possibilities offered by this technology, before trying to fully optimize the process.

Some studies, however, propose some interesting strategies to increase the yield. For instance, Jia, *et al.*, [86] obtained 48.2g of boric acid from synthetic radioactive wastewater using vacuum membrane distillation crystallization, *i.e.*, a 50% recovery of boric acid in the original solution. They further stated that they could have continued the concentration up to a theoretical recovery rate of 72% using **multi-stage** vacuum membrane distillation-crystallization. Edwie, *et al.*, [77] recovered 10.3 kg NaCl per m^3 by cooling the crystallization tank after it had reached supersaturation using membrane distillation. In a subsequent study, the same research group [57] studied simultaneous membrane distillation-crystallization and observed that increasing the feed **temperature** leads to higher yield (up to 34 kg NaCl per m^3 of feed solution). It is interesting to note that this yield is consequently higher than in their previous work [77] thanks to the simultaneous membrane distillation-crystallization technique that is dependent on the amount of evaporated solvent and not solely on the different operating temperatures as in the case of non-simultaneous MD and crystallization. Li, *et al*., [87] attained 34.2 to 40.5% of Na_2CO_3 recovery and 50.7 to 54% of Na_2SO_4 recovery, and mentioned that **membrane blockage** must be avoided in order to improve this yield. Finally, Yan, *et al*., [88] showed that seeding could increase the crystal production rate.

Another interesting observation from the reviewed literature (Table 3) is that there is no commonly accepted method to calculate the yield. Several calculations have been reported: i) the ratio between the actual yield to that of the theoretical yield; ii) the ratio between the produced salt mass and the mass of remaining mother liquor; iii) the ratio between the recovered and the initially dissolved mass of crystals; iv) the ratio between the amount of recovered crystals and the initial amount of feed solution; v) the mass of crystals recovered per m^3 of produced water, *etc*. Hence, although the instrument of measure is invariably a simple balance, this variety of yield definitions lowers the representativeness of the values reported in different studies. In order to facilitate comparisons, it would be interesting to uniformize the calculation and define the percent yield Y_P as it is usually defined for crystallization processes:

$$Y_P = \frac{w_p}{Y_T} \cdot 100\% \qquad 2$$

With w_p the weight of the product, and Y_T [kg] the theoretical crystal yield calculated as follows [2], [54]:

$$Y_T = w\,R\,\frac{C_1 - C_2(1-V)}{1 - C_2(R-1)} \qquad 3$$

With C_1 [kg anhydrous salt/kg solvent] the initial solution concentration, C_2 [kg anhydrous salt/kg solvent] the final solution concentration, w the initial mass of solvent [kg], R the ratio of molar masses hydrated crystal and anhydrous crystals, and V [kg per kg of original solvent] the solvent lost by evaporation.

Table 3: Main studies reporting crystal yield obtained via membrane distillation-crystallization.

Target recovery	Membrane	Config.	Scale	Yield	Instrument of measure	Ref.
NaCl	Tubular, PP	SGMD	Laboratory	1 to 2%, ratio between the produced salt mass and the mass of remaining mother liquor.	/	[38]
NaCl	Hollow fiber, PVDF	DCMD	Laboratory	Increasing the feed temperature leads to higher yield (up to 34 kg NaCl per m^3 feed solution.	Balance	[57]
NaCl	Hollow fiber, PP and PVDF	DCMD	Laboratory	At recovery factor of 37%, 16.4 kg NaCl recovered per m^3 water recovered.	Balance	[58]
$CaCO_3$ and NaCl	Hollow fiber, PP	DCMD	Laboratory	Solid production rate up to 2.72 kg/m^2/day.	/	[65]
NaCl	Hollow fiber, PP	DCMD	Bench	21 kg NaCl/m^3 artificial RO brine after 3h of supersaturation.	Balance	[70]
Na_2SO_4	Flat sheet, PVDF	DCMD	Laboratory	38% of the initially dissolved amount of salts, *i.e.*, near to 100 kg/m^3.	Analytical balance	[76]
NaCl	Hollow fiber, PVDF	DCMD	Laboratory	Recovery up to 10.3 kg/m^3 with cooling. Feed = 27 wt.% at 60°C.	Balance	[77]
NaCl	Hollow fiber, PTFE	Submerged VMD	Laboratory	31.85%, *i.e.*, 31.85 g of the 100 g initially dissolved.	Electronic balance	[78]
Struvite ($MgNH_4PO_4\,H_2O$)	Flat sheet, PVDF modified	DCMD	Laboratory	Around 82% of phosphate recovery.	/	[81]
Struvite ($MgNH_4PO_4\,H_2O$)	Hollow fiber, PP	DCMD	Laboratory	Around 60% of phosphorus recovery.	/	[82]
NaCl	Hollow fiber, PVDF	DCMD	Laboratory	Yield of 64 g per kg feed.	/	[83]
$CaCO_3$ + $MgCO_3$	Hollow fiber, PP	Submerged VMD	Laboratory	Up to 16.14 g produced on a theoretical 35.9 g maximum crystal production.	Balance	[84]
L-ascorbicacid	Hollow fiber, PVDF	SGMD	Bench	27%, ratio between the actual yield to that of the theoretical yield.	/	[85]
Boric acid	Hollow fiber, PP	VMD	Laboratory	48.2g, *i.e.*, 50% of boric acid in the original solution.	/	[86]
Na_2CO_3 and Na_2SO_4	Hollow fiber, PP	OMD	Laboratory	34.2% to 40.5% Na2CO3 recovery. 50.7% to 54% Na_2SO_4 recovery.	/	[87]
NH_4NO_3	Hollow fiber, PP and flat sheet, ePTFE	DCMD	Bench	40% of the initial salt mass.	/	[89]
Gypsum	Flat sheet, PVDF	DCMD	Laboratory	Crystal production rate increases (12 to 16 $kgm^{-3}d^{-1}$) with increasing seeding dose.	Mass balance of calcium.	[88]

3.4 Crystal purity

Crystal purity is an indication of the level of possible contaminations, responsible for the distortion of the crystal features and morphology [90]. Among the membrane distillation-

crystallization studies mentioning the purity of the obtained crystals (Table 4), Jia, *et al.*, [86] reported a boric acid purity over 99% with trace amounts of nuclides during vacuum membrane distillation-crystallization of boric acid from simulated radioactive wastewater. Ali, *et al.*, [58] used direct contact membrane distillation-crystallization for NaCl recovery from produced water and reported a purity higher than 99.9%. Quist-Jensen, *et al.*, [82] studied direct contact membrane distillation-crystallization of struvite from real wastewater and detected low traces of impurities such as calcium and iron. Kim, *et al.*, [65] first identified 94.4% calcite and 5.6% halite during direct contact membrane distillation-crystallization, and 99.9% halite in a later stage, most probably due to the higher supersaturation ratio. Li, *et al.*, [87] reached a purity of more than 97% using osmotic membrane distillation-crystallization, with mainly Cl- impurities because of its use as osmotic agent. Therefore, using the osmotic membrane distillation configuration may not be the best choice when a high purity is desired. However, Ye, *et al.*, [91] obtained the same purity as commercial Na_2CO_3 powders, i.e., reaching up to 99.5%, using osmotic membrane distillation-crystallization. Salmon, *et al.*, [48] also used osmotic membrane distillation-crystallization and recovered super high-purity crystals hence OMD can be an option but must be perfectly controlled to avoid wetting.

Overall, considering that fine chemicals usually require a purity >99% [92], membrane distillation-crystallization is competitive with the conventional technologies thanks to its ability to produce high-purity crystals. Weckesser, *et al.*, [38] demonstrated this competitivity when they obtained 99.71 to 99.94% NaCl purity in membrane crystallization from saturated synthetic NaCl/KCl solution versus 99.58% in vacuum evaporation. They marked a better purification potential via multistage centrifugation/washing in membrane distillation than in vacuum evaporation, which is likely due to the difference in growth rate.

It must be noted that several studies reported here use X-Ray diffraction (XRD) solely to determine the crystal purity. However, this technique only allows a semi-quantitative analysis whose results must be interpreted carefully. Indeed, the peak intensity of the XRD pattern is a function of the amount of the phase present in the sample, but also of the sample preparation (non-random crystallite orientation), the degree of crystallinity and the crystal size [93]. Therefore, elemental analysis such as energy-dispersive X-ray spectroscopy or inductively coupled plasma should be performed as complementary analysis in order to confirm the atomic or weight percentage of each element [94].

Table 4: Main studies reporting crystal purity obtained via membrane distillation-crystallization.

Target recovery	**Membrane**	**Config.**	**Feed solution**	**Purity**	**Instrument of measure**	**Ref.**
NaCl	Tubular, PP	SGMD	Saturated synthetic NaCl/KCl solution.	99.71 to 99.94% in membrane crystallization versus 99.58% in vacuum evaporation.	Ion chromatography	[38]
Na_2CO_3	Hollow fiber, PP	OMD	Synthetic wastewater of Na_2CO_3, Na_2SO_4 and KNO_3.	High purity, no co-crystallization.	XRD	[48]
NaCl	Hollow fiber, PP and PVDF	DCMD	Produced water from KISR, containing 248 g/L of TDS.	> 99.9%.	XRD	[58]
$CaCO_3$ and NaCl	Hollow fiber, PP	DCMD	Shale gas produced water collected from multi-wells.	94.4% calcite ($CaCO_3$) and 5.6% halite (NaCl) (earlier stage) and 99.9% halite (NaCl) (later stage).	XRD	[65]
Struvite ($MgNH_4PO_4 H_2O$)	Hollow fiber, PP	DCMD	Wastewater from Aaby wastewater treatment plant.	Low proportions of impurities.	XRD, ICP-OES analysis	[82]
Boric acid	Hollow fiber, PP	VMD	Synthetic radioactive wastewater.	>99%.	Dissolving the recovered boric acid in deionized	[86]

					water, analyzing concentration	
Na_2CO_3 and Na_2SO_4	Hollow fiber, PP	OMD	Synthetic Na_2SO_4 and Na_2CO_3 solutions.	>97%.	ICS-2000 ion chromatography	[87]
Na_2CO_3	Hollow fiber, PP	OMD	Synthetic alkaline solution obtained after CO_2 absorption, with NaCl, $NaNO_3$ and Na_2SO_4 impurities.	Up to 99.5% with washing. Impurities adsorbed on the surface of the crystals.	XRD	[91]

3.5 Crystal nucleation and growth rates

Understanding the crystallization phenomenon compulsory requires the study of the two main processes intervening during crystallization, namely nucleation and growth. Both phenomena are usually interconnected during conventional crystallization processes, but membrane distillation can offer the possibility to distinguish between them by inducing nucleation on the membrane and proceed with further growth in a separate crystallizer. This was experimented by Jiang, *et al.*, [51] who obtained a nucleation rate one to two orders of magnitude higher at the surface of the membrane than in the bulk. If the crystals then detach and end up in the bulk, growth would be preferred over homogeneous nucleation because of the low supersaturation level. Therefore, nucleation would happen dominantly in the membrane, and growth mostly in the bulk.

In order to calculate the nucleation and growth rates, most of the studies [45], [49], [51], [58], [62]–[64], [72], [75], [95], [96] calculate semi-empirical values using the **Randolph-Larson general-population balance**:

$$\frac{dn}{dL} + \frac{n}{Gt} = 0 \qquad 4$$

Integrating between n_0 and n, the population density of initial nuclei (size L = 0) and that of size L respectively, it becomes:

$$\ln(n) = -\frac{L}{Gt} + \ln(n^0) \text{ or } n = n^0 \exp\left(-\frac{L}{Gt}\right) \qquad 5$$

$$B^0 = n^0 G \qquad 6$$

With n the crystal population density, L the crystal size, G the growth rate, t the retention time, n^0 the initial population density. The underlying assumptions are steady-state operation, solids-free feed, well-mixed suspension and negligible crystal breakage [61]. Under these conditions, a plot of $\ln(n)$ versus L should give a straight regression line whose slope is $-1/Gt$ and whose intercept with the ordinate axis is $\ln(n^0)$. The growth and nucleation rates directly follow.

Other studies are based on the **measure of the growth rate** [57], [69], [70]: when defining the growth rate as $G = \Delta L/\Delta t$, experimental values can be obtained for G, most often via camera monitoring. When defining the nucleation rate as $B = \Delta n/\Delta t$, experimental values can also be obtained for B, most often via crystal size distribution measurement and correlation with total mass of crystals. Edwie, *et al.*, [57] describe these calculations in detail. Having determined the nucleation and growth rate experimentally, some studies retrieve kinetic parameters (k_G and g) from the classical nucleation and growth theory [69], [70]:

$$G = k_G(c - c^*)^g \qquad 7$$

$$B = k_B G^b \text{ or } B = a \exp\left(-\frac{d}{ln(S^2)}\right) \qquad 8$$

With k_G the kinetic rate constant for G, k_B the nucleation rate constant, c the actual salt concentration, c^* the solubility, and g the growth rate order. S is the supersaturation, a is a pre-exponential factor, and d is a constant. Also, the driving force $(c - c^*)$ can be experimentally determined. Then, equation (1) can be rewritten as:

$$\log(G) = \log(k_G) + g\,\log(c - c^*) \qquad 9$$

Again, a plot of $\log(G)$ versus $\log(c - c^*)$ should give a straight regression line whose slope is g and whose intercept with the ordinate axis is $\log(k_G)$.

Finally, Jiang [39], [43], [51] uses another approach involving the computation of the **nucleation work**, where some parameters are similarly obtained by fitting the experimental data.

Studies on measured and simulated growth and nucleation rates (Table 5) show that a slower growth rate is obtained with membrane distillation-crystallization as opposed to **conventional technologies**. Weckessern *et al.*, [38] reported a higher growth rate with vacuum evaporation; Jiang, *et al.*, [39] reported higher growth rate with conventional cooling crystallization, and Qu, *et al.*, [67] reported a higher growth rate with conventional evaporation crystallization.

Several authors studied the influence of operating conditions on growth rate. Quist-Jensen, *et al.*, [42] and Ali, *et al.*, [58] reported a decreasing growth rate with increasing **flow rate**. However, Curcio, *et al.*, [44] observed an increase in growth rate with flow velocity followed by a decrease. Quist-Jensen, *et al.*, [63] on the other hand, reported a larger growth rate at higher flow rate. The effect of **temperature** is also quite disparate: Jiang, *et al.*, [43] observed that diffusion-controlled growth rate increases with temperature. Similarly, Ali, *et al.*, [58] reported an increasing growth rate with increasing temperature, but Edwie, *et al.*, [57] witnessed a decreasing growth rate with increasing feed temperature. Likewise, Kim, *et al.*, [65] reported a decreasing growth rate with increasing crystallizer temperature. The presence of **impurities** usually decreases the growth rate of crystals [44], [75], [91] except for the work of Macedonio, *et al.*, [49] where the NaCl growth rate has accelerated when strontium was present in the feed solution. The **membrane type** was also reported to influence growth rate in different manners. Tsai, *et al.*, [96] reported a higher growth rate with membranes made of PVDF than of PP. On the contrary Ali, *et al.*, [58] concluded that the growth rate with PVDF membranes is lower than with PP ones. Macedonio, *et al.*, [45] reported a higher growth rate with PVDF-Bi_2Se_3 membranes than with common pristine PVDF membranes. Perotta, *et al.*, [62] observed the highest growth rate with PVDF/Graphene Platelet, 5%. Ko, *et al.*, [95] compared PMSQ tubular aerogel membranes obtained via a sol-gel process (CM-L) with alumina hollow fiber membranes obtained via phase-inversion and sintering (CM-S). They concluded that the growth rate was faster with CM-S because of the higher transmembrane flux. Cui, *et al.*, [64] concluded in their study that the highest surface porosity and pore size was responsible for the highest growth rate. Finally, other parameters were also found to influence the growth rate: Quist-Jensen, *et al.*, [72] report decreasing growth rate with **time**, and Julian, *et al.*, [84] report that **vibration and aeration** increase growth rate on the membrane.

Nucleation rate was less studied than growth rate. Amongst the few existing studies, Edwie, *et al.*, [57] reported that the nucleation rate increases with increasing feed **temperature**. However, Kim, *et al.*, [65] showed that the nucleation rate decreases when the temperature of the crystallizer increases. Meng, *et al.*, [97] found out that some nucleation sites are preferential on virgin **membrane** but that the sites are more regular on their modified membranes. Jiang, *et al.*, [39] pointed out that PP membranes result in higher nucleation work than PVDF membranes with the same porosity. They also concluded from their simulations that increasing the porosity leads to lower nucleation work. Julian, *et al.*, [84] reported a $CaCO_3$ nucleation rate without thermal **water softening** 13 times higher than with thermal water softening.

In this section, the review of the literature identified several variables that can have an effect on the growth and nucleation rates. In general, the growth rate in membrane distillation-crystallization was reported to be slower than with conventional processes. Some studies report the influence of the temperature and flow rate on nucleation and growth rate, but the results are disparate as this is influenced by the specific process conditions and the compound to be crystallized. The presence of impurities, membrane type, vibration and aeration were also found to influence the growth rate hence these parameters could also be tuned to improve the control of growth and nucleation rate.

Table 5: Main studies reporting crystal nucleation and growth rates during the membrane distillation-crystallization process.

Target recovery	**Membrane**	**Config.**	**Nucleation rate B**	**Growth rate G**	**Measurement**	**Ref.**
NaCl	Tubular, PP	SGMD	/	Higher growth rate in vacuum evaporation leading to impure crystals. 5.0 10^{-10} to 5.4 10^{-10} for MC, 3 10^{-8} for vacuum evaporation.	Photosedimentation. Total crystallite mass measured. G calculated from the measured mass growth rate, with CSD and dm.	[38]
KNO_3	Hollow fiber, PP	DCMD	PP: higher nucleation work than PVDF with same porosity. Increasing porosity leads to lower work.	2.27 10^{-7} m/s conventional cooling, 1.98 10^{-7} m/s DCMD.	Preliminary experimental data fitting.	[39]
LiCl	Hollow fiber, PP	VMD	/	0.0323 - 0.824 µm/min for feed temperature around 38°C. Decreases with the increase of flow rate.	Suspension samples. Optical microscope, camera and image analysis.	[42]
NaCl	Hollow fiber, PP	VMD	Heterogeneous nucleation rate between 0 and 0.37 [mol m^{-3} min^{-1}].	Diffusion controlled growth rate increases with temperature, up to 1.81 10^{-7} m/s.	Previous experimental data fitting.	[43]
Hen egg white	Hollow fiber, PP	OMD	/	Increase with flow velocity, till a maximum of 2.5 10^{-10} m/s, then decrease. Decrease with integration of impurities.	Samples collected at various time intervals. Optical microscope, camera. Growth rate calculated as function of the number of molecules precipitated and the flux of molecules towards a growing crystal.	[44]
NaCl	Flat sheet, hybrid PVDF-Bi_2Se_3	DCMD	/	6.98 10^{-4} mm/min (PVDF-Bi_2Se_3) vs 5.74 10^{-4} mm/min (pristine PVDF).	Optical microscope. Randolph-Larson.	[45]
NaCl	Hollow fiber, PP	DCMD	/	0.0511 without, 0.054 with strontium. Higher when strontium is present.	Solution samples withdrawn at 0-, 30- and 60-min. Screen analysis via video microscope. Randolph-Larson.	[49]
NaCl	Hollow fiber, PP	VMD	~ 10^{14} [# m^{-3} s^{-1}]. at the membrane surface, and ~10^{14} [# m^{-3} s^{-1}] in the bulk. One to two orders	0-0.35 µm s^{-1} at the membrane surface, depending on the viscosity (measured and simulated).	Particle vision measurement to obtain in situ images of crystals in the crystallizer. Previous	[51]

			of magnitude higher at surface.		experimental data fitting.	
NaCl	Hollow fiber, PP	DCMD	B_0 = 7.3 10^{18} $MG^{2.08}$ (M=slurry density, G=growth rate).	2.33 10^{-3} µm/s.	Suspension samples. Screen analysis via video microscope. Randolph – Larson.	[56]
NaCl	Hollow fiber, PVDF	DCMD	2.21 10^9 to 3.4 10^{10} [# m^{-3}] from 40°C to 70°C feed temperature. Increases with increasing feed temperature. Dominates growth at high temperature.	1.36 to 2.43 10^{-8} m/s from 70°C to 40°C feed temperature. Decreases with increasing feed temperature.	Suspension samples withdrawn at predetermined residence time. Optical microscope, digital camera, image analysis software. Mass of crystals correlated with CSD to find number of crystals.	[57]
NaCl	Hollow fiber, PP and PVDF	DCMD	/	Growth rate increases with temperature (0.03 to 0.16 µm/min for PP, 0.005 to 0.03 µm/min for PVDF), but decreases with feed flow rate (0.04-0.16 µm/min). Growth rate with PVDF is lower than with PP.	Samples of mother liquid containing crystals. Microscope, video camera and image analysis. Randolph-Larson.	[58]
$MgSO_4$ and NaCl	Hollow fiber, PP	DCMD	/	1.6 10^{-8} m/s for epsomite.	Suspension samples. Microscopic visualization of CSD (camera).	[60]
NaCl	Flat sheet PVDF and graphene	DCMD	Molecular simulations indicate a multi-pathway nucleation.	Higher growth rate for PVDF/Graphene Platelet5% (1.6 10^{-4} mm/min).	Feed samples taken from crystallization tank. Optical microscope, camera. Randolph-Larson.	[62]
$MgSO_4$	Hollow fiber, PDVF	DCMD	/	Growth rate larger at high flow rate (0.1 to 0.4 µm/min from low to high flow rate).	Samples extracted from feed tank. Optical microscope. Randolph-Larson.	[63]
NaCl	Flat sheet, Hyflon/PVDF	DCMD	/	0.0118 to 0.046 µm/min. Highest surface porosity and pore size responsible for highest growth rate.	Solution samples withdrawn every 30 min. Microscope analysis. Randolph-Larson.	[64]
$CaCO_3$ and NaCl	Hollow fiber, PP	DCMD	2.94 10^5 to 11.2 10^5 [# m^{-3} s^{-1}]. Influenced by the "seeding effect". Decreases when crystallizer temperature increases. Increase when feed velocity increases.	0.403 10^{-8} to 4.74 10^{-8} m/s. Influenced by the "seeding effect". Decreases when crystallizer temperature increases.	Crystal samples formed in a crystallizer. SEM.	[65]
$MgSO_4$	Hollow fiber, PP	VMD	5.1 10^{10} to 4.38 10^{11} [# m^{-3} s^{-1}].	Slightly lower than conventional.	/	[67]
Na_2SO_4	Hollow fiber, PP	DCMD	/	1.56 10^{-8} m/s.	Suspension samples taken out every 30 min. Optical-microscope, image analysis.	[68]
NaCl	Hollow fiber, PVDF	DCMD	B = -9.73 10^{11} $G^{-0.83}$ [# $s^{-1}m^{-3}$].	G = 1.0002 10^2 $\Delta c^{1.415}$ m/s.	Crystals appearing on the membrane peeled	[69]

					off by ultrasonic cleaner at several times, granulometry, data regression.	
NaCl	Hollow fiber, PP	DCMD	Ln B [# $m^{-3}s^{-1}$] = 14 to 18. The total number of crystals generated from natural brines was in average 27% lower than that observed when using an artificial retentate.	0.8-2.5 10^{-8} m/s, for real seawater RO brines, reduction of 15-23% with respect to that measured on artificial concentrates. g = 0.56 (natural seawater) to 0.6 (artificial seawater).	Suspension samples every 30 min. Experimental measurement of solution concentration and density curves. Optical microscope.	[70]
Na_2SO_4	Hollow fiber, PP	DCMD	9189-13862 [# L^{-1} min^{-1}].	0.5310-0.6014 µm/min. Decreases with time.	Suspension samples every 30 min. Optical microscope, image analysis. Randolph-Larson.	[72]
NaCl	/	DCMD	/	0.04 - 0.16 µm/min. Growth rate is smaller with RO than NF brines. The presence of humic acid lowers the growth rate.	Suspension samples withdrawn every 30 min. Optical microscope, camera, screen analysis. Randolph-Larson.	[75]
$CaCO_3$ + $MgCO_3$	Hollow fiber, PP	Submerged VMD	Aeration is responsible for additional heterogeneous nucleation. Vibration can limit crystal deposition on the membrane. $CaCO_3$ nucleation rate without thermal water softening: 0.011068 [#/h/µm^2], 13 times higher than with thermal water softening (0.000815 [#/h/m^2]).	Vibration and aeration increase membrane growth rate. Vibration can limit growth on the membrane.	Evaluation of crystal deposition on the surface using SEM and EDS. Nucleation rate computed with time, crystal number density and fractional membrane area covered by crystals.	[84]
Na_2CO_3	Hollow fiber, PP	OMD	No influence of impurities on nucleation.	NO_3^- and Cl^- had no effect. SO_4^{2-} slowed down the growth rate.	Suspension samples at outlet of membrane and in tank. Microscope images.	[91]
NaCl and LiCl	Hollow fiber, ceramic	VMD	CM-L: NaCl: 55203 to 802.583 [# L^{-1} min^{-1}] CM-S: NaCl: 35544 to 156580 [# L^{-1} min^{-1}].	CM-L: NaCl: 0.01609 to 0.09023 µm/min. CM-S: NaCl: 0.23 to 0.594 µm/min. Faster growth rate with CM-S because of the higher transmembrane flux.	Feed samples removed at regular intervals. Optical microscope. Randolph-Larson.	[95]
NaCl	Tubular, PP and PVDF	DCMD	/	6.5 10^{-5} to 2.2 10^{-4} mm/min PVDF and 2.5 to 5.7 10^{-5} mm/min PP. Hence just slightly higher in PVDF than in PP.	Suspension samples every 30 min. Pictures recorded with a video camera module with optical head. Randolph-Larson.	[96]
NaCl	Hollow fiber PP, flat sheet PTFE with superhydro	DCMD and VMD	Some nucleation sites are preferential on virgin membrane. Modified membrane: more even.	/	Microscope, video camera. Analysis of crystals deposited on the membrane surface.	[97]

	phobic modificatio ns					

3.6 Induction time

The induction time of a crystallization process is usually defined as the period elapsed between the achievement of supersaturation and the detection of the first crystals [54]. As nucleation occurs at the nanometer scale, this induction time is not really the nucleation time since critical-sized nuclei are hardly detectable. Many parameters such as supersaturation level, mixing, heat effects, impurities, and viscosity are known to influence induction times of conventional crystallization processes [98]. At very low supersaturation, the latent period is defined as the onset of a significant change in the system, e.g., the occurrence of massive nucleation [54]. At high supersaturation, induction time and latent period overlap. The induction time is technique-dependent hence it is a parameter hardly comparable [99]. The measurement devices differ mostly by their cost and precision, going from simple visual inspection to more elaborated techniques such as light scattering, electron microscopy, nuclear magnetic resonance and fluorescence [100]. The induction time is commonly studied for crystallization, and membranes could be of great interest as they could reduce this induction time thanks to the facilitated heterogeneous nucleation.

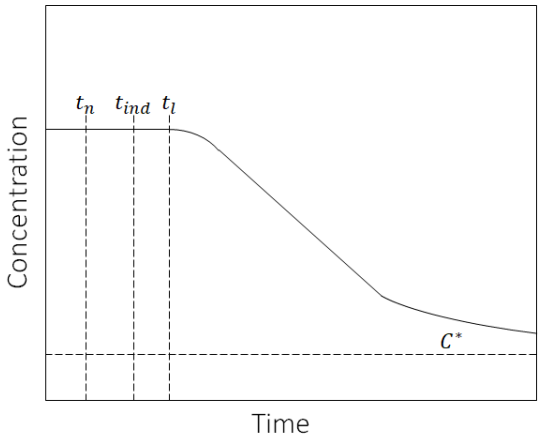

Figure 3: Typical desupersaturation curve, with t_n the nucleation time, t_{ind} the induction time t_l the latent period and C the saturation concentration. Adapted from [Mullin].*

Very few membrane distillation-crystallization studies report induction times or latent periods, and these terms are not always appropriately used. Among others, Julian, *et al.*, [84] observed the "induction time for severe fouling" in the case of submerged vacuum membrane distillation-crystallization and reported higher values when using air bubbles aeration. Di Profio, *et al.*, [40] reported induction times of 64h to 17.5h depending on the rate of solvent evaporation. Perrotta, *et al.*, [62] performed molecular dynamics simulations with experimental validation and reported shorter induction times when using graphene loaded PVDF membranes than using pristine PVDF membranes. Di Profio, *et al.*, [41] studied static and dynamic osmotic membrane distillation-crystallization and observed that the induction time lowers with lower feed velocity. Quist-Jensen, *et al.*, [63] also witnessed that nucleation occurs earlier at higher flow rate. Cui, *et al.*, [64] needed 322 to 1267 minutes for reaching crystals formation using direct contact membrane distillation-crystallization with three different PVDF membranes. The shortest crystals formation time was observed with the membrane having the highest surface porosity and pore size. Tsai, *et al.*, [96] needed 360 min for detecting and recovering crystals with PVDF membrane, and from 165 to 283 min with PP membrane. Finally, Cui, *et al.*, [64] concluded that high surface porosity and pore size was responsible for a reduction of nucleation time.

As a conclusion, although very few studies reported result about induction times or latent periods, the few parameters that were reported to have an influence include the use of air bubbles aeration, the rate of solvent evaporation, the type of membrane, the feed velocity and the flow rate.

4. Scaling and strategies for its mitigation

Membrane scaling is induced by the deposition of salts, oxides, and hydroxides, which eventually reduces the transmembrane flux and facilitates membrane wetting. In membrane distillation-crystallization, this phenomenon may be significant as the membrane is in direct contact with highly concentrated salt solutions. Nevertheless, it must be avoided as much as possible since it leads to the decrease of transmembrane flux, requiring frequent cleaning procedures, which could produce membrane deterioration [32]. In order to minimize scaling, the use of seeding has been proposed to promote bulk crystallization instead of surface crystallization [67], [101], [102]. However, crystallization on the membrane surface is also an opportunity since the membrane can be used as a heterogeneous nucleation site to promote controlled nucleation of crystals. Ideally, crystal detachment thanks to the flow shear stress should follow to conduct the nuclei to a separate crystallizer for further growth. However, this is not easily performed in practice, and the risk of membrane scaling and blockage is high. Strategies to control crystallization on the membrane while resisting undesirable scaling take mainly three directions, similar to the scaling mitigation strategies in regular membrane distillation processes:

(i) **Feed pretreatment:** In membrane distillation, efforts have been made to remove compounds prone to scaling prior to operation. Hsieh *et al.*, [103] investigated different conventional pretreatment methods of hypersaline water (filtration, oxidation, coagulation, airfloatation and aeration), and found that ultrafiltration and coagulation showed the best anti-scaling results. The use of alginate and calcium, fouling precursors, with stream resulting from seawater treatment, also appeared to have some anti-scaling effect and enhanced water flux [104]. Aeration and acidification of brine feed stream, work well together, in removing the total inorganic carbon and limiting the saturation of calcium carbonate [105]. Zhang *et al.*, [106] used barium to allow for barite precipitation and the removal of sulfite from brackish water. Overall, depending on the feed composition/ source (wastewater, ground water, seawater, etc.), an adequate pretreatment (aeration, ultrafiltration, adsorption, dosing antiscalants, coagulation, etc.) is conducted to hinder the scaling effect. In membrane distillation-*crystallization*, if a feed stream contains multiple salts, a first strategy to mitigate scaling would be the removal of the undesirable salts prior to the crystallization step. Besides, this can also have positive impacts on the crystal morphology.

(ii) **Control of operating conditions:** Hydrodynamic control at the membrane interface has been practiced with the introduction of ultrasonication, air bubble or turbulence [107]. Pulse flow was shown to have an impact on the scaling behavior as it provides vibrations of the membrane and fluid turbulence that disrupt aggregation and deposition of the particles on the surface [105]. The operating temperature has also been investigated such that a high temperature hinders the solubility of ions, which results in faster formation of large crystals at the surface of the membrane [108]. Aside from that, increasing the feed flow velocity is recommended for more of bulk crystallization, rather than crystallization at the membrane surface, which gives less tendency towards scaling [109]. Also, the feed flow velocity and viscosity were shown to be important operating parameter to transit from scaling to nucleation regulation via controlled crystal detachment from the membrane [51].

(iii) **Membrane modification:** In regular membrane distillation, scaling problems have been overcome using membrane with a self-cleaning ability; notably, the superhydrophobic or

omniphobic membranes. The addition of ZnO nanowires for example endorsed further hydrophobicity into the membrane. The presence of these nanofibers represented a barrier to heterogeneous nucleation, and reduced the contact area and time between the fluid and the membrane surface [102]. Liu *et al.*, [107] showed that a porous hydrophobic membrane of low surface porosity requires more energy for heterogeneous nucleation, so thermodynamically, the membrane has the lowest possibility to form surface scaling. However, in membrane distillation-*crystallization*, heterogeneous nucleation can be desired to some extent. Therefore, research also shows modified membranes providing some preferred nucleation sites whence crystals could detach easily. In this regard, Meng *et al.*, [97] showed that some membranes induce localized crystal nucleation and deposition, leading to isolated pillars of salt crystals with further crystal growth. Perrotta *et al.*, presented that nanocomposite membranes can direct the nucleation and growth of NaCl crystals depending on the loading of the fillers. Jiang, et al., [51] has conducted modelling and experimental study about the mechanisms of heterogeneous nucleation on the membrane and crystal detachment. They reported the possibility of interface-based crystal particle auto selection and detachment for nucleation regulation and control.

Implementing strategies to mitigate the scaling effect on the performance of membrane distillation-crystallization technology would allow for gaining the full potential of the technology with robust and durable processes. Besides the strategies abovementioned, a better understanding of the kinetic mechanisms governing crystal nucleation and growth influenced by the membrane is necessary, particularly that this step occurs at the nanometer scale and is a probabilistic process [33], [96]. More research in this direction must be encouraged.

5. Recent advances in membrane distillation-crystallization and critical remarks

Membrane distillation-crystallization has come a long way since its introduction in 1987, in terms of both process improvement and understanding of the role of the membrane [8]. Nowadays, research is mainly focusing on three main topics:

i) Development of **new process configurations**: several variants such as percrystallization, submerged vacuum membrane distillation and membrane distillation integrated with hollow-fiber cooling crystallization have been investigated [8]. Percrystallization is a membrane separation technique in which both the solute and the solvent permeate through the membrane pores. As the permeate side is under vacuum, the crystals detach from the membrane and are recovered simultaneously with the solvent [110]. This configuration could help solving the scaling problem encountered in membrane crystallization, but it yields relatively smaller crystals [111]. Membrane distillation integrated with hollow fiber cooling crystallization makes use of two different membranes during the crystallization process. This configuration could ease the scaling-up of the process, but the scaling problems on the surface of the membrane remain an issue [83]. Finally, submerged vacuum membrane distillation-crystallization is the variant that still receives the most attention nowadays [112]–[115]. This configuration is attractive as it suppresses the need for feed recirculation, and it offers the possibility of intensification via stirring and aeration [78]. However, it discards the advantage of separated nucleation and growth offered by membrane distillation-crystallization compared to conventional crystallizers. Future research directions in terms of process configurations will most likely be driven by the scaling problem. Some researchers imagine feed pre-treatments to reduce scaling, whereas others try to improve crystal detachment from the membrane (percrystallization, stirring, aeration, use of ultrasounds, *etc.*). Improvement of the process configurations for an improved scaling control could allow the technology to move forward and gain full potential.

ii) **Molecular dynamics** simulations have been recently applied to membrane distillation-crystallization in order to go deeper in the understanding of the fundamental mechanisms behind crystallization induced by a membrane [96] [116] [117]. These studies demonstrate the importance of the membranes in assisting the crystal growth, speeding up the nucleation, and affecting the crystal morphology. Different membrane compositions [116] and feed composition [117] were studied, and were demonstrated to be key parameters for crystallization control. Molecular dynamics have thus shown their relevance in the field of membrane distillation-crystallization and may become a valuable tool for crystallization understanding and control. However, the operating conditions vary along the membrane and affect the crystallization process, but this has not been taken into account yet. Therefore, coupling molecular dynamics to CFD modelling could be of great interest.

iii) Finally, an emerging topic in membrane distillation-crystallization is the **modification of the membrane** characteristics for improved crystallization control. Several authors focus on improving the transmembrane flux, which can lead to an increased crystal recovery [81], [118] . Others focus on membrane surface modification, which influences the crystal growth and nucleation [116]. This research direction should be encouraged as it embraces the full membrane potential for crystallization control via membrane distillation-crystallization. Moreover, modifying the membranes to provide some preferred nucleation sites whence crystals could detach easily may tackle the scaling problem encountered in membrane distillation-crystallization, as described in section 4.

All of these latest research topics have in common the desire to control the crystallization process. This objective has already been aimed for in numerous previous membrane distillation-crystallization studies, and will undoubtedly still be aimed for in the future. Several other topics will also need more attention in order to bring this technology to maturity:

i) Very few attempts of **CFD modeling** of membrane crystallization are reported in the literature even though this has already been highlighted by several authors [7], [119]. Although membrane distillation has already been significantly modeled using CFD, membrane distillation-crystallization seems to be left behind. This could be because crystallization introduces a solid phase which thus requires multi-phase flow analysis and a deep knowledge of computational fluid dynamics. The statistical nature of nucleation and growth processes may also act as a brake, as complex phenomena such as nuclei dissolution, agglomeration and breakage must be considered. However, CFD modelling would increase the understanding of the process and would be an insightful tool for membrane module design, process design, and crystallization control. More research endeavors should be devoted to this specific topic.

ii) Further developments are needed for the **scaling up and the development of a continuous crystallization process**. Several studies [33] consider the possibility of a continuous process with crystal nucleation on the membrane followed by detachment and then further growth in a separate crystallizer. However, continuous membrane distillation-crystallization is still an important challenge and the development of an efficient crystal recovery system would be needed [8]. Above that, the intrinsic easy scale-up advantage of membranes is compromised by the need of a separate crystallizer for crystal growth. Indeed, it is well-known that the scale-up of crystallization vessels is a very complex task because of the interrelated geometry, degree of supersaturation and mixing parameters [4]. If a crystallizer vessel is needed in the process, the easy scale up claimed by many authors studying membrane distillation-crystallization becomes inaccurate [83]. However, if the membrane can work on its own, the easy scale up would indeed be an outstanding asset for membrane distillation-crystallization [30], [120].

6. Conclusions and perspectives

This review highlights the influence of different variables in membrane distillation-crystallization on the control of crystal morphology, crystal size distribution, crystal yield, crystal purity, nucleation and growth rates, and process induction time. The main findings of this study are summarized below:

i. The **crystal morphology** was demonstrated to be influenced by the supersaturation (hence controlled by evaporation rate and temperature), the process conditions (flow rate, microwaves, *etc.*) and the presence of impurities. Therefore, membrane distillation-crystallization coupled to well-chosen pre-treatment step would be an excellent combination for applications such as recovery of high-quality crystals from waste streams.

ii. The **crystal size distribution** (CSD) is usually represented by the mean diameter and coefficient of variation. Generally, the coefficient of variation reported in most of the membrane distillation-crystallization studies were found to be relatively low compared to conventional MSMPR crystallization that usually yields crystals with a coefficient of variation of 50%. Investigations about the influence of time on the crystal size distribution most often reported increasing the coefficient of variation (CV) and mean diameters with time with some exceptions explained by secondary nucleation in the crystallization plant. The membrane seems to have also an effect on the CSD hence the crystallization of a certain compound could be optimized by choosing an appropriate membrane with adequate fillers. Influence of the temperature and flow rate on CSD and CV is dependent on the specific process and compound to be crystallized. Seeding, stirring rate, aeration, and microwave radiation were found to also be able to tune the CSD but more studies are needed to determine if this applies to all membrane distillation-crystallization configurations and compounds. However, all these operating parameters undeniably have an impact and can be optimized for a specific process.

iii. **Crystal yield** in membrane distillation-crystallization is quite low compared to conventional crystallization. Some studies propose though some interesting leads to increase the yield. For instance, using a multi-stage process [86], using simultaneous membrane distillation-crystallization rather than non-simultaneous membrane distillation-crystallization [77], and optimizing the process to avoid membrane blockage [87]. Another interesting observation emerging from this review is that there is no commonly accepted method to calculate the yield hence it is difficult to compare the results. Therefore, a common percent yield calculation is proposed.

iv. Several studies showed that membrane distillation-crystallization can ensure a high **crystal purity**. However, it must be noted that most of the studies use X-Ray diffraction solely to determine the crystal purity, but this technique only allows a semi-quantitative analysis whose results must be interpreted carefully. Therefore, a complementary elemental analysis should be performed in order to consolidate the results.

v. **Nucleation and growth rate** are either calculated semi-empirically using the Randolph-Larson general-population balance or purely empirically. Membrane distillation offers the possibility to distinguish the two phenomena by inducing nucleation on the membrane, proceeded with further growth in a separate crystallizer [51]. Also, the growth rate is generally lower than in conventional crystallization. Similar to CSD, the influence of the temperature and flow rate on nucleation and growth rate depends on the specific process conditions and compound to be crystallized. The presence of impurities, membrane type, vibration and aeration were also found to influence the nucleation and growth rate.

vi. Very few membrane distillation-crystallization studies report **induction times** or latent periods, and these terms are not always appropriately used. Some studies report the influence of air bubbles aeration, rate of solvent evaporation, membrane characteristics and feed velocity. However, comparison between studies is difficult because of the different definitions for the reference time.

As a general conclusion, membrane distillation-crystallization was proven to be a high-performing candidate for crystallization control. Indeed, a multitude of process parameters can be tuned to enable a precise control of crystal morphology, crystal size distribution, crystal yield, crystal purity, nucleation and growth rates, and process induction time. Several studies already demonstrated the influence of various parameters and research is still on-going to further improve the crystallization control. However, it is of crucial importance that researchers harmonize their ways of defining and calculating the different crystallization properties. Finally, in order to accelerate the development of this promising technology, future research should focus on CFD modelling, continue with the development of modified membranes to reduce scaling and improve crystallization control, and ultimately tackle the challenges of scaling up and developing a continuous process.

Acknowledgements

The authors acknowledge the support of the Université Catholique de Louvain (UCLouvain) and of the European Research Council (ERC) for the ERC Starting Grant UE H2020 CO2LIFE 759630.

Funding

This work was supported by the European Research Council (ERC) under the European Union's Horizon 2020 research and innovation programme (grant agreement ERC Starting Grant UE H2020 CO2LIFE 759630), and the Université Catholique de Louvain (UCLouvain).

Declaration of Competing Interests

The authors have no competing interests to declare.

Bibliography

[1] A. Lewis, M. Seckler, H. Kramer, and G. van Rosmalen, *Industrial Crystallization: Fundamentals and Applications*. Cambridge University Press, 2015.

[2] S. R. Anderson *et al.*, *Handbook of industrial crystallization*. .

[3] H. Lu, J. Wang, T. Wang, N. Wang, Y. Bao, and H. Hao, "Crystallization techniques in wastewater treatment: An overview of applications," *Chemosphere*, vol. 173, pp. 474–484, 2017.

[4] S. Vedantam and V. V. Ranade, "Crystallization: Key thermodynamic, kinetic and hydrodynamic aspects," *Sadhana - Acad. Proc. Eng. Sci.*, vol. 38, no. 6, pp. 1287–1337, 2013.

[5] Y. Ma, S. Wu, E. G. J. Macaringue, T. Zhang, J. Gong, and J. Wang, "Recent Progress in Continuous Crystallization of Pharmaceutical Products: Precise Preparation and Control," *Org. Process Res. Dev.*, vol. 24, no. 10, pp. 1785–1801, 2020.

[6] L. G. Benning, *New Perspectives on Mineral Nucleation and Growth*. 2017.

[7] E. Chabanon, D. Mangin, and C. Charcosset, "Membranes and crystallization processes: State of the art and prospects," *J. Memb. Sci.*, vol. 509, pp. 57–67, 2016.

[8] A. Ali *et al.*, "A review of membrane crystallization, forward osmosis and membrane capacitive deionization for liquid mining," *Resour. Conserv. Recycl.*, no. August, 2020.

[9] M. C. Sparenberg, I. Ruiz Salmón, and P. Luis, "Economic evaluation of salt recovery from wastewater via membrane distillation-crystallization," *Sep. Purif. Technol.*, vol. 235, no. April 2019, p. 116075, 2020.

[10] P. Das, S. Dutta, and K. K. Singh, "Insights into membrane crystallization: A sustainable tool for value added product recovery from effluent streams," *Sep. Purif. Technol.*, vol. 257, no. July 2020, p. 117666, 2021.

[11] E. Curcio and E. Drioli, "Membrane distillation and related operations - A review," *Sep. Purif. Rev.*, vol. 34, no. 1, pp. 35–86, 2005.

[12] E. Drioli, A. Ali, and F. Macedonio, "Membrane distillation : Recent developments and perspectives," *Desalination*, vol. 356, pp. 56–84, 2015.

[13] A. Gugliuzza and A. Basile, *Membrane contactors: Fundamentals, membrane materials and key operations*, vol. 2. Woodhead Publishing Limited, 2013.

[14] I. A. Said, T. Chomiak, J. Floyd, and Q. Li, “Sweeping gas membrane distillation (SGMD) for wastewater treatment, concentration, and desalination: A comprehensive review,” *Chem. Eng. Process. - Process Intensif.*, vol. 153, no. January, p. 107960, 2020.

[15] A. Alkhudhiri, N. Darwish, and N. Hilal, “Membrane distillation : A comprehensive review,” *Desalination*, vol. 287, pp. 2–18, 2012.

[16] M.-C. Sparenberg, B. Hanot, C. Molina Fernandez, and P. Luis, “Experimental mass transfer comparison between vacuum and direct contact membrane distillation for the concentration of carbonate solutions,” *Sep. Purif. Technol.*, vol. 275, no. June, p. 119193, 2021.

[17] G. Naidu, L. Tijing, M. A. H. Johir, H. Shon, and S. Vigneswaran, “Hybrid membrane distillation: Resource, nutrient and energy recovery,” *J. Memb. Sci.*, vol. 599, no. May 2019, p. 117832, 2020.

[18] Y. Q. Xiong, T. Peng, and Z. F. Shi, “Research progress and enhancement of MDC process,” *Adv. Mater. Res.*, vol. 955–959, pp. 2530–2533, 2014.

[19] P. Luis, *Fundamental Modeling of Membrane Systems: Membrane and Process Performance*. Elsevier Science, 2018.

[20] S. Palosaari, M. Louhi-kultanen, and Z. Sha, “Industrial Crystallization,” in *Handbook of Industrial Drying*, 2006, pp. 1203–1223.

[21] R. Lakerveld, J. Kuhn, H. J. M. Kramer, P. J. Jansens, and J. Grievink, “Membrane assisted crystallization using reverse osmosis : Influence of solubility characteristics on experimental application and energy saving potential,” *Chem. Eng. Sci.*, vol. 65, no. 9, pp. 2689–2699, 2010.

[22] X. Zhou *et al.*, “Continuous production of drug nanocrystals by porous hollow fiber-based anti-solvent crystallization,” *J. Memb. Sci.*, vol. 564, no. April, pp. 682–690, 2018.

[23] D. M. Zarkadas and K. K. Sirkar, “Solid Hollow Fiber Cooling Crystallization,” pp. 7163–7180, 2004.

[24] Y. Choi, G. Naidu, L. D. Nghiem, S. Lee, and S. Vigneswaran, “Membrane distillation crystallization for brine mining and zero liquid discharge: opportunities, challenges, and recent progress,” *Environ. Sci. Water Res. Technol.*, pp. 1202–1221, 2019.

[25] E. Drioli, G. Di Profio, and E. Curcio, “Progress in membrane crystallization,” *Curr. Opin. Chem. Eng.*, vol. 1, no. 2, pp. 178–182.

[26] G. Di Profio, E. Curcio, and E. Drioli, “Supersaturation Control and Heterogeneous Nucleation in Membrane Crystallizers : Facts and Perspectives,” *Ind. Eng. Chem. Res.*, pp. 11878–11889, 2010.

[27] E. Curcio, G. Di Profio, and E. Drioli, “Microporous hydrophobic Membranes for crystallization of biomolecules,” *Chem. Eng. Trans.*, vol. 47, no. 2, pp. 421–426, 2016.

[28] C. Charcosset, R. Kieffer, D. Mangin, D. Lyon, F.- Lyon, and V. Uni, “Coupling between Membrane Processes and Crystallization Operations,” *Ind. Eng. Chem. Res.*, pp. 5489–5495, 2010.

[29] X. Jiang, Y. Shao, L. Sheng, P. Li, and G. He, “Membrane Crystallization for Process Intensification and Control: A Review,” *Engineering*, vol. 7, no. 1, pp. 50–62, 2021.

[30] D. Zhang, S. Xu, S. Du, J. Wang, and J. Gong, “Progress of Pharmaceutical Continuous Crystallization,” *Engineering*, vol. 3, no. 3, pp. 354–364, 2017.

[31] I. Ruiz Salmón and P. Luis, “Membrane crystallization via membrane distillation,” *Chem. Eng. Process. Process Intensif.*, vol. 123, no. June 2017, pp. 258–271, 2018.

[32] B. Kumar, P. Kandasamy, and T. Li, “A critical review of membrane crystallization for the purification of water and recovery of minerals,” *Rev. Environ. Sci. Biotechnol.*, pp. 411–439, 2016.

[33] X. Jiang, L. Tuo, D. Lu, B. Hou, W. Chen, and G. He, “Progress in membrane distillation crystallization: Process models, crystallization control and innovative applications,” *Front. Chem. Sci. Eng.*, vol. 11, no. 4, pp. 647–662, 2017.

[34] E. Drioli, A. Criscuoli, and E. Curcio, *Membrane Contactors: Fundamentals, Applications and Potentialities*. Elsevier Science, 2011.

[35] E. Drioli, “European Roadmap of Process Intensification -Technology Report – Technology: Membrane Crystallization Technology.”

[36] J. Haleblian and W. McCrone, “Pharmaceutical applications of polymorphism,” *J. Pharm. Sci.*,

vol. 58, no. 8, pp. 911–929, 1969.
[37] D. Lu, P. Li, W. Xiao, G. He, and X. Jiang, “Simultaneous Recovery and Crystallization Control of Saline Organic Wastewater by Membrane Distillation Crystallization,” *AIChE J.*, vol. 63, no. 6, 2017.
[38] D. Weckesser and A. König, “Particle shape and purity in membrane based crystallization,” *Chem. Eng. Technol.*, vol. 31, no. 1, pp. 157–162, 2008.
[39] X. Jiang, D. Lu, W. Xiao, X. Ruan, J. Fang, and G. He, “Membrane Assisted Cooling Crystallization : Process Model , Nucleation , Metastable Zone , and Crystal Size Distribution,” *AIChE J.*, vol. 62, no. 3, 2016.
[40] G. Di Profio, S. Tucci, E. Curcio, and E. Drioli, “Controlling Polymorphism with Membrane-Based Crystallizers : Application to Form I and II of Paracetamol,” *Chem. Mater.*, no. 5, pp. 2386–2388, 2007.
[41] G. Di Profio, “Selective Glycine Polymorph Crystallization by Using Microporous Membranes,” *Cryst. Growth Des.*, vol. 7, no. 3, pp. 526–530, 2007.
[42] C. A. Quist-Jensen, A. Ali, S. Mondal, F. Macedonio, and E. Drioli, “A study of membrane distillation and crystallization for lithium recovery from high-concentrated aqueous solutions,” *J. Memb. Sci.*, vol. 505, pp. 167–173, 2016.
[43] X. Jiang *et al.*, “Hybrid Control Mechanism of Crystal Morphology Modi fi cation for Ternary Solution Treatment via Membrane Assisted Crystallization,” *Cryst. Growth Des.*, 2018.
[44] E. Curcio, S. Simone, G. Di Profio, E. Drioli, A. Cassetta, and D. Lamba, “Membrane crystallization of lysozyme under forced solution flow,” *J. Memb. Sci.*, vol. 257, no. 1–2, pp. 134–143, 2005.
[45] F. Macedonio, A. Politano, E. Drioli, and A. Gugliuzza, “Bi2Se3-assisted membrane crystallization,” *Mater. Horizons*, vol. 5, no. 5, pp. 912–919, 2018.
[46] Z. Ji, J. Wang, Z. Yin, D. Hou, and Z. Luan, “Effect of microwave irradiation on typical inorganic salts crystallization in membrane distillation process,” *J. Memb. Sci.*, vol. 455, pp. 24–30, 2014.
[47] W. Ye, J. Lin, J. Shen, P. Luis, and B. Van Der Bruggen, “Membrane crystallization of sodium carbonate for carbon dioxide recovery: Effect of impurities on the crystal morphology,” *Cryst. Growth Des.*, vol. 13, no. 6, pp. 2362–2372, 2013.
[48] I. R. Salmón, K. Simon, C. Clérin, and P. Luis, “Salt Recovery from Wastewater Using Membrane Distillation-Crystallization,” *Cryst. Growth Des.*, 2018.
[49] F. Macedonio *et al.*, “Thermodynamic modeling of brine and its use in membrane crystallizer,” *Desalination*, vol. 323, pp. 83–92, 2013.
[50] F. Macedonio and E. Drioli, “Hydrophobic membranes for salts recovery from desalination plants,” *Desalin. Water Treat.*, vol. 18, no. 1–3, pp. 224–234, 2010.
[51] X. Jiang, “Interface-Based Crystal Particle Autoselection via Membrane Crystallization : From Scaling to Process Control,” *AIChE J.*, vol. 65, no. 2, pp. 723–733, 2019.
[52] A. Caridi, G. Di Profio, R. Caliandro, A. Guagliardi, E. Curcio, and E. Drioli, “Selecting the desired solid form by membrane crystallizers: Crystals or cocrystals,” *Cryst. Growth Des.*, vol. 12, no. 9, pp. 4349–4356, 2012.
[53] P. M. Doran, “Chapter 11 - Unit Operations,” in *Bioprocess Engineering Principles (Second Edition)*, Second Edi., P. M. Doran, Ed. London: Academic Press, 2013, pp. 445–595.
[54] J. W. Mullin, *Crystallization*, 4th ed. 2001.
[55] A. Chianese, “Characterization of Crystal Size Distribution,” pp. 1–6, 2012.
[56] E. Curcio, A. Criscuoli, and E. Drioli, “Membrane Crystallizers,” pp. 2679–2684, 2001.
[57] F. Edwie and T. S. Chung, “Development of simultaneous membrane distillation-crystallization (SMDC) technology for treatment of saturated brine,” *Chem. Eng. Sci.*, vol. 98, pp. 160–172, 2013.
[58] A. Ali, C. A. Quist-Jensen, F. Macedonio, and E. Drioli, “Application of membrane crystallization for minerals’ recovery from produced water,” *Membranes (Basel).*, vol. 5, no. 4, pp. 772–792, 2015.
[59] M. Frappa, F. Macedonio, A. Gugliuzza, W. Jin, and E. Drioli, “Performance of PVDF Based Membranes with 2D Materials for Membrane Assisted-Crystallization Process,” *Membranes*

(Basel)., pp. 1–16, 2021.
[60] L. Mariah *et al.*, "Membrane distillation of concentrated brines — Role of water activities in the evaluation of driving force," *J. Memb. Sci.*, vol. 280, pp. 937–947, 2006.
[61] A. Ali and C. A. Quist-Jensen, "Membrane operations for minerals' recovery from seawater," in *Current Trends and Future Developments on (Bio-) Membranes*, Elsevier Inc., 2018, pp. 449–471.
[62] M. L. Perrotta, F. Macedonio, E. Tocci, L. Giorno, E. Drioli, and A. Gugliuzza, "Graphene stimulates the nucleation and growth rate of nacl crystals from hypersaline solution via membrane crystallization†," *Environ. Sci. Water Res. Technol.*, vol. 6, no. 6, pp. 1723–1736, 2020.
[63] C. A. Quist-Jensen, F. Macedonio, and E. Drioli, "Membrane crystallization for salts recovery from brine—an experimental and theoretical analysis," *Desalin. Water Treat.*, vol. 57, no. 16, pp. 7593–7603, 2016.
[64] Z. Cui *et al.*, "Testing of three different PVDF membranes in membrane assisted-crystallization process: Influence of membrane structural-properties on process performance," *Desalination*, vol. 440, no. December 2017, pp. 68–77, 2018.
[65] J. Kim, J. Kim, and S. Hong, "Recovery of water and minerals from shale gas produced water by membrane distillation crystallization," *Water Res.*, vol. 129, pp. 447–459, 2018.
[66] P. M. Doran, *Bioprocess Engineering Principles*. Elsevier Science, 2012.
[67] M. Qu, S. You, and L. Wang, "Insights into nucleation and growth kinetics in seeded vacuum membrane distillation crystallization," *J. Memb. Sci.*, no. July, p. 118813, 2020.
[68] E. Curcio *et al.*, "Hybrid nanofiltration – membrane crystallization system for the treatment of sulfate wastes," *J. Memb. Sci.*, vol. 360, no. 1–2, pp. 493–498, 2010.
[69] G. Chen, Y. Lu, X. Yang, R. Wang, and A. G. Fane, "Quantitative Study on Crystallization-Induced Scaling in High- Concentration Direct-Contact Membrane Distillation," *Ind. Eng. Chem. Res.*, 2014.
[70] X. Ji, E. Curcio, S. Al, G. Di, E. Fontananova, and E. Drioli, "Membrane distillation-crystallization of seawater reverse osmosis brines," *Sep. Purif. Technol.*, vol. 71, pp. 76–82, 2010.
[71] M. T. Chan, A. G. Fane, J. T. Matheickal, and R. Sheikholeslami, "Membrane distillation crystallization of concentrated salts - Flux and crystal formation," *J. Memb. Sci.*, vol. 257, no. 1–2, pp. 144–155, 2005.
[72] C. A. Quist-Jensen, F. Macedonio, D. Horbez, and E. Drioli, "Reclamation of sodium sulfate from industrial wastewater by using membrane distillation and membrane crystallization," *Desalination*, vol. 401, pp. 112–119, 2017.
[73] Y. Shin and J. Sohn, "Mechanisms for scale formation in simultaneous membrane distillation crystallization: Effect of flow rate," *J. Ind. Eng. Chem.*, vol. 35, pp. 318–324, 2016.
[74] G. Chen, Y. Lu, W. B. Krantz, R. Wang, and A. G. Fane, "Optimization of operating conditions for a continuous membrane distillation crystallization process with zero salty water discharge," *J. Memb. Sci.*, vol. 450, pp. 1–11, 2014.
[75] F. Macedonio and E. Drioli, "Hydrophobie membranes for salts recovery from desalination plants," *Desalin. Water Treat.*, 2010.
[76] R. Bouchrit, A. Boubakri, T. Mosbahi, A. Ha, and S. A. Bouguecha, "Membrane crystallization for mineral recovery from saline solution : Study case Na 2 SO 4 crystals Membrane crystallization for mineral recovery from saline solution : Study case Na 2 SO 4 crystals," *Desalination*, vol. 412, no. February, pp. 1–12, 2017.
[77] F. Edwie and T. S. Chung, "Development of hollow fiber membranes for water and salt recovery from highly concentrated brine via direct contact membrane distillation and crystallization," *J. Memb. Sci.*, vol. 421–422, pp. 111–123, 2012.
[78] T. Zou, G. Kang, M. Zhou, M. Li, and Y. Cao, "Submerged vacuum membrane distillation crystallization (S-VMDC) with turbulent intensification for the concentration of NaCl solution," *Sep. Purif. Technol.*, vol. 211, no. June 2018, pp. 151–161, 2019.
[79] B. Journal, Y. N. Nariyoshi, C. E. Pantoja, and M. M. Seckler, "EVALUATION OF SODIUM

CHLORIDE CRYSTALLIZATION IN MEMBRANE DISTILLATION CRYSTALLIZATION APPLIED TO WATER DESALINATION," *Brazilian J. Chem. Eng.*, vol. 33, no. 03, pp. 675–690, 2016.

[80] A. Cerda *et al.*, "Recovering water from lithium-rich brines by a fractionation process based on membrane distillation-crystallization," *J. Water Process Eng.*, vol. 41, no. March, 2021.

[81] H. Tan, W. Tan, B. S. Ooi, and C. P. Leo, "Superhydrophobic PVDF / micro fibrillated cellulose membrane for membrane distillation crystallization of struvite," *Chem. Eng. Res. Des.*, vol. 0, pp. 54–68, 2021.

[82] C. A. Quist-Jensen *et al.*, "Membrane crystallization for phosphorus recovery and ammonia stripping from reject water from sludge dewatering process," *Desalination*, vol. 440, no. November 2017, pp. 156–160, 2018.

[83] L. Luo, J. Zhao, and T. S. Chung, "Integration of membrane distillation (MD) and solid hollow fiber cooling crystallization (SHFCC) systems for simultaneous production of water and salt crystals," *J. Memb. Sci.*, vol. 564, no. June, pp. 905–915, 2018.

[84] H. Julian, S. Meng, H. Li, Y. Ye, and V. Chen, "Effect of operation parameters on the mass transfer and fouling in submerged vacuum membrane distillation crystallization (VMDC) for inland brine water treatment," *J. Memb. Sci.*, vol. 520, pp. 679–692, 2016.

[85] F. Anisi, K. M. Thomas, and H. J. M. Kramer, "Membrane-assisted crystallization: Membrane characterization, modelling and experiments," *Chem. Eng. Sci.*, vol. 158, no. June 2016, pp. 277–286, 2017.

[86] F. Jia, J. Li, and J. Wang, "Recovery of boric acid from the simulated radioactive wastewater by vacuum membrane distillation crystallization," *Ann. Nucl. Energy*, vol. 110, pp. 1148–1155, 2017.

[87] W. Li, B. Van der Bruggen, and P. Luis, "Recovery of Na2CO3 and Na2SO4 from mixed solutions by membrane crystallization," *Chem. Eng. Res. Des.*, vol. 106, pp. 315–326, 2016.

[88] Z. Yan *et al.*, "Integration of seeding- and heating-induced crystallization with membrane distillation for membrane gypsum scaling and wetting control," *Desalination*, vol. 511, no. April, p. 115115, 2021.

[89] J. A. Bush *et al.*, "Membrane distillation crystallization of ammonium nitrate solutions to enable sustainable cold storage: Electrical conductivity as an in-situ saturation indicator," *J. Memb. Sci.*, vol. 631, no. April, 2021.

[90] E. Drioli and L. Giorno, *Encyclopedia of Membranes*. Springer Berlin Heidelberg, 2014.

[91] W. Ye, J. Lin, J. Shen, P. Luis, and B. Van Der Bruggen, "Membrane Crystallization of Sodium Carbonate for Carbon Dioxide Recovery : Effect of Impurities on the Crystal Morphology," *Cryst. Growth Des.*, 2013.

[92] W. Beckmann and A. Kramer, *Crystallization Basic Concepts and Industrial Applications*. Wiley, 2013.

[93] J. R. Connolly and X. P. Diffraction, "Introduction Quantitative X-Ray Diffraction Methods," pp. 1–15, 2012.

[94] M. Bortolotti, L. Lutterotti, and G. Pepponi, "Combining XRD and XRF analysis in one Rietveld-like fitting," *Powder Diffr.*, vol. 32, no. S1, pp. S225–S230, 2017.

[95] C. C. Ko *et al.*, "Performance of ceramic membrane in vacuum membrane distillation and in vacuum membrane crystallization," *Desalination*, vol. 440, no. March, pp. 48–58, 2018.

[96] J. Tsai *et al.*, "Membrane-Assisted Crystallization : A Molecular View of NaCl Nucleation and Growth," *Appl. Sci.*

[97] S. Meng, Y. Ye, J. Mansouri, and V. Chen, "Crystallization behavior of salts during membrane distillation with hydrophobic and superhydrophobic capillary membranes," *J. Memb. Sci.*, vol. 473, pp. 165–176, 2015.

[98] H. N. Kim and K. S. Suslick, "The effects of ultrasound on crystals: Sonocrystallization and sonofragmentation," *Crystals*, vol. 8, no. 7, 2018.

[99] D. Kashchiev and G. M. Van Rosmalen, "Review: Nucleation in solutions revisited," *Cryst. Res. Technol.*, vol. 38, no. 7–8, pp. 555–574, 2003.

[100] A. Bernardo, C. E. Calmanovici, and E. A. Miranda, "Induction time as an instrument to enhance

comprehension of protein crystallization," *Cryst. Growth Des.*, vol. 4, no. 4, pp. 799–805, 2004.
[101] Z. Yan *et al.*, "Integration of seeding-and-heatinginduced crystallization with membrane distillation for membrane gypsum scaling and wetting control," *Desalination*, vol. 511, 2021.
[102] T. Pan *et al.*, "ZnO Nanowires@PVDF nanofiber membrane with superhydrophobicity for enhanced anti-wetting and anti-scaling properties in membrane distillation," *J. Memb. Sci.*, vol. 621, no. October 2020, 2021.
[103] I. M. Hsieh, A. K. Thakur, and M. Malmali, "Comparative analysis of various pretreatments to mitigate fouling and scaling in membrane distillation," *Desalination*, vol. 509, no. October 2020, 2021.
[104] E. Arkhangelsky, F. Wicaksana, and R. Wang, "Anti-scaling and water flux enhancing effect of alginate in membrane distillation," *Desalination*, vol. 514, no. May, 2021.
[105] G. Viader *et al.*, "Integration of membrane distillation as volume reduction technology for in-land desalination brines management: Pre-treatments and scaling limitations," *J. Environ. Manage.*, vol. 289, no. April, 2021.
[106] Z. Zhang, O. R. Lokoare, A. V. Gusa, and R. D. Vidic, "Pretreatment of brackish water reverse osmosis (BWRO) concentrate to enhance water recovery in inland desalination plants by direct contact membrane distillation (DCMD)," *Desalination*, vol. 508, no. January, 2021.
[107] L. Liu *et al.*, "Understanding the fouling/scaling resistance of superhydrophobic/omniphobic membranes in membrane distillation," *Desalination*, vol. 499, no. October 2020, 2021.
[108] A. Bauer, M. Wagner, H. Horn, and F. Saravia, "Operation conditions affecting scale formation in membrane distillation - An in situ scale study based on optical coherence tomography," *J. Memb. Sci.*, vol. 623, no. October 2020, 2021.
[109] G. Naidu, S. Jeong, and S. Vigneswaran, "Influence of feed/permeate velocity on scaling development in a direct contact membrane distillation," *Sep. Purif. Technol.*, vol. 125, no. February, pp. 291–300, 2014.
[110] Y. Meng, K. Li, L. Yu, Y. Zhang, H. Liu, and J. Wang, "Preliminary study on a novel vacuum membrane percrystallization process [新型真空膜渗透结晶工艺初探]," *Chinese J. Environ. Eng.*, vol. 15, no. 7, pp. 2314–2321, 2021.
[111] J. Motuzas *et al.*, "Novel inorganic membrane for the percrystallization of mineral, food and pharmaceutical compounds," *J. Memb. Sci.*, vol. 550, pp. 407–415, 2018.
[112] H. Julian, H. Rizqullah, M. A. Siahaan, and I. G. Wenten, "Cane sugar crystallization using submerged vacuum membrane distillation crystallization (SVMDC)," *J. Food Sci. Technol.*, no. 1, 2020.
[113] Y. Choi, G. Naidu, S. Lee, and S. Vigneswaran, "Recovery of sodium sulfate from seawater brine using fractional submerged membrane distillation crystallizer," *Chemosphere*, vol. 238, p. 124641, 2020.
[114] Y. Choi, G. Naidu, S. Jeong, S. Lee, and S. Vigneswaran, "Fractional-submerged membrane distillation crystallizer (F-SMDC) for treatment of high salinity solution," *Desalination*, vol. 440, no. August 2017, pp. 59–67, 2018.
[115] Y. S. Chang *et al.*, "Microalgal exopolymeric substances fouling in submerged vacuum membrane distillation and its mitigation via enhanced air bubbling," *Desalination*, vol. 508, no. March, p. 115047, 2021.
[116] M. L. Perrotta *et al.*, "Molecular insights on NaCl crystal formation approaching PVDF membranes functionalized with graphene," *Phys. Chem. Chem. Phys.*, vol. 22, no. 15, pp. 7817–7827, 2020.
[117] P. Li *et al.*, "Na+/Mg2+ interactions on membrane distillation permeation flux and crystallization performance during high saline solution treatment," *Sep. Purif. Technol.*, vol. 259, 2021.
[118] M. Nasiraee, S. M. Mousavi, E. Saljoughi, S. Kiani, and K. Razmgar, "Production of calcium nitrate crystals via membrane distillation crystallization using polyvinylidene fluoride/sorbitan trioleate membranes," *Adv. Powder Technol.*, no. xxxx, 2021.
[119] X. Jiang, Y. Shao, L. Sheng, P. Li, and G. He, "Membrane Crystallization for Process Intensification

and Control : A Review," *Engineering*, 2020.
[120] G. Di Profio, E. Curcio, and E. Drioli, "Membrane Crystallization Technology," in *Comprehensive Membrane Science and Engineering*, vol. 4, 2010, pp. 21–46.